Formability Characterisation of Tri-Ply Cladded Sheet Metal of Stainless Steel with Aluminium in Core

A
Project Report

submitted in fulfillment for the award of the degree of

MASTER OF TECHNOLOGY

in

Production and Industrial Engineering

Department of Mechanical Engineering

Delhi Technological University

Under Guidance of:

Mr. VIJAY GAUTAM

(ASSISTANT PROFESSOR)

Submitted by :

BIJENDRA PRASAD

2K14/PIE/04

Department of Mechanical Engineering

Delhi Technological University

Delhi

CERTIFICATE

This is to certify that the thesis entitled **"Formability Characterisation of Tri-ply cladded sheet metal of Stainless steel with Aluminum in core"** submitted by **Bijendra Prasad (2K14/PIE/04)**, during the session 2014-2016 for the award of M.Tech degree of Delhi Technological University, Delhi is absolutely based upon his work done under my supervision and guidance and that neither this thesis nor any part of it has been submitted for any degree/diploma or any other academic award.

Mr. Vijay Gautam

Assistant Professor

Department of Mechanical Engineering

Delhi Technological University

Delhi

ACKNOWLEDGEMENT

I would like to take this opportunity to express my deep sense of respect and gratitude to my project guide Mr. Vijay Gautam, Assistant Professor, Department of Mechanical Engineering, Delhi Technological University, Delhi for his invaluable and fruitful constructive suggestions and guidance that have enabled me to overcome all the problems and difficulties in this project. His untiring devotion, noble guidance, valuable suggestions and above all continuous encouragement played an important role in the completion of this project.

I would like thank Dr. D.Ravi Kumar , Professor, Mechanical Engineering Dept, IIT Delhi for giving me permission to conduct experiment at sheet metal lab at IIT Delhi.

I would like to thank Dr. Vikas Rastogi, Professor, Mechanical Engineering Dept, DTU for allowing me to conduct Finite element analysis in Design Centre Lab, DTU.

I would like to thank the in charge of Metal forming lab, Mechanical Engineering Dept, DTU Mr. Tekchand and Mr. Omprakash for their help in extending all facility required for my experiments.

I have great pleasure in thanking Mr Satish and Mr. VedPrakash, research scholar at IIT Delhi for their kind help in conducting the experiments in sheet metal Lab.

Finally I would say special thanks to my parents, my mentor and god for their endless love, understanding, encouragement, patience and support during my study.

Bijendra Prasad

ABSTRACT

Today Clad sheet metals is seen to have their increasing popularity in various industrial applications like in automobile body parts, cookware manufacture, aerospace applications etc. the clad sheets have enhanced mechanical properties over the individual component of the clad sheet. They tend to increase strength, ductility, thermal conductivity, surface properties and contribute in overall reduction of weight.

This present study is confined to a roll bonded tri-ply cladded sheet of AISI304 on one side AISI430 on other with AA1050 sandwiched in between them having combined thickness of 2.5mm. Firstly the peel strength the roll bond was tested as per ASTM-D1876 standard. The tensile specimens were laser cut in three different directions 0^0, 45^0 and 90^0 with rolling direction(RD) as per ASTM-E8M standard. The tensile properties like UTS, yield strength, ductility and strain hardening of clad sheet and individual sheets are tested and compared. The drawability of the clad sheet is determined by performing anisotropy test and determined the *R* value (Lankford value) in directions 0^0, 45^0 and 90^0 with rolling direction(RD) . All these tests are performed on 50kN Universal testing machine.

The forming limit diagram(FLD) for the clad sheet is drawn by performing limit dome height(LDH) test on 100 tonne hydraulic press using 50mm hemispherical punch. The specimens are laser cut in dog bone shape in various widths from 20mm to 100mm. Die, holder and punch are fabricated by CNC milling from AISI D2 tool steel. A circular grid of 2.5mm diameter is laser etched on all the specimens for measurement of major and minor strains. The necking strains on the deformed circles were measured on the tested specimens and a forming limit diagram was plotted. Finite Element analysis is also carried out and the experimental results are found to be in good agreement with the FE results.

Keywords: Tri-ply Cladded Sheet Metal, Cold Roll Bonding, Forming Limit Diagram, Finite Element Analysis

DECLARATION

I, **Bijendra Prasad**, hereby certify that the work which is being presented in the Major Project entitled **"Formability Characterisation of Tri-ply cladded sheet metal of Stainless steel with Aluminum in core"**, is submitted, in the fulfillment of the requirements for degree of Master of Technology at Delhi Technological University is an authentic record of my own work carried under the supervision of **Mr. Vijay Gautam**. I have not submitted the matter embodied in this seminar for the award of any other degree or diploma also it has not been directly copied from any source without giving its proper reference.

Bijendra Prasad
2K14/PIE/04
M.Tech (Production and Industrial Engineering)
Delhi Technological University

LIST OF FIGURES

LIST OF TABLES

CONTENTS

NOMENCLATURE

σ	True stress
ϵ	True strain
s	Engineering stress
e	Engineering strain
n	Strain hardening coefficient
K	Strength coefficient
R	Plastic strain ratio
R_0 R_{45} and R_{90}	Anisotropic value in 0^o, 45^o and 90^o to the rolling direction
R_{avg}	Average plastic strain ratio or Normal anisotropy
t	Sheet thickness.
ϵ_1	Major principal strain
ϵ_2	Minor principal strain

CHAPTER – 1
INTRODUCTION

1.1 Sheet metals and its applications

Sheet metals are formed by an industrial process into thin, flat pieces which can be cut and bent into a variety of shapes. Countless day to day objects are constructed using sheet metals. Sheet metal is available in flat pieces or coiled strips. The coils are produced by running a continuous sheet of metal through a roll slitter.

There are many different metals that can be made into sheet metal, such as brass, aluminum, copper, steel, tin, nickel and titanium. For decorative uses, important sheet metals include gold, silver, and platinum are considered. Sheet metal are usually used for car body panels, airplane wings, building roofs, food and drink cans, domestic home appliances and many other applications.

1.2 Clad Sheet Metals

Now-a-days, clad metallic materials, consisting of two or more layers, are being used in various industrial fields because of their unique corrosion resistance, specific strength, and surface properties. Clad sheets get enhanced physical properties compared to the individual sheets used for making the clad sheet.

There are several solid-state bonding methods to make the clad sheets such as diffusion, explosive and cold roll bonding(CRB). Among them, the cold roll bonding technique is the most common process because it is cost effective and efficient. Multi-layered clad sheets can be fabricated. These sheets are designed to possess high strength, good thermal conductivity, anti-corrosion properties, wear resistance, surface quality, and so forth (N.V.Govindaraj, 2013). In general, clad metals can be produced by several processes, for instance, explosive bonding, adhesive bonding, or cold/ hot roll bonding (Akbarzadeh, 2015) .The cold roll-bonding process is the most efficient and cost effective in which sheet metals are bonded together by interface diffusion, while the thickness is reduced by a rolling process followed by annealing (Kim, 2013). The cold roll-bonding process has many advantages, especially accurate dimension control and straight bonding layers (Yu, 1997). The most widely fabricated clad sheets are Al/Cu, Al/Fe, Al/ferritic stainless steel, Al/Mg/Al , AZ31/Al/ferritic stainless steel, austenitic stainless

steel/Al/Cu, Ti/steel/Ti, and Ti/ferritic stainless steel (H.C.Tseng, 2010) (I.K. Kim, 2014). Clad sheet metals find applications in automotive parts like in exhaust system, cooking utensils, electromagnetic cookers, structural panels.

1.3 Important Sheet Metal Forming Processes

Sheet metal forming processes are those where force is applied on a piece of sheet metal to modify its geometry rather than remove any material. The applied force stresses the metal beyond its yield strength, causing the material to plastically deform, but not to fail. By doing so, the sheet can be bent or stretched into a variety of complex shapes. Different types of sheet metal forming processes are discussed here below along with their applications:

1.3.1 Roll Forming

The process is performed on a roll forming line in which the sheet metal stock is fed through a series of roll stations as show in Fig. 1.1. Each station has a roller, referred to as a roller die, positioned on both sides of the sheet. The shape and size of the roller die may be unique to that station, or several identical roller dies may be used in different positions. The roller dies may be above and below the sheet, along the sides, at an angle, etc. As the sheet is forced through the roller dies in each roll station, it plastically deforms and bends. Each roll station performs one stage in the complete bending of the sheet to form the desired part. The roller dies are lubricated to reduce friction between the die and the sheet, thus reducing the tool wear. Also, lubricant can allow for a higher production rate, which will also depend on the material thickness, number of roll stations, and radius of each bend. Rolling is suitable for mass production with constant cross section and long sheet metal parts, they also have low production cost.

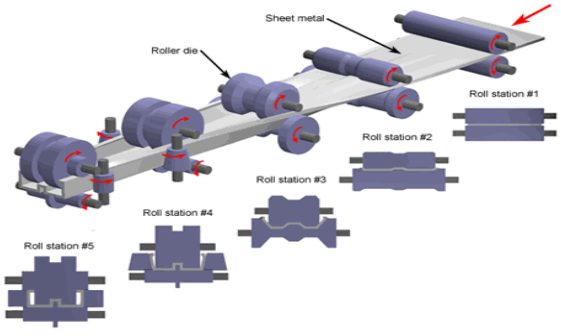

Fig 1.1 Roll Forming Line (CustomPartNet, 2009)

1.3.2 Deep Drawing

Deep drawing is a metal forming process in which sheet metal is stretched into the desired part shape. A tool pushes downward on the sheet metal, forcing it into a die cavity in the shape of the desired part. The tensile forces applied to the sheet cause it to plastically deform into a cup-shaped part. Deep drawn parts are characterized by a depth equal to more than half of the diameter of the part. These parts can have a variety of cross sections with straight, tapered, or even curved walls, but cylindrical or rectangular parts are most common. Deep drawing is most effective with ductile metals, such as aluminum, brass, copper, and mild steel. Examples of parts formed with deep drawing include automotive bodies and fuel tanks, cans, cups, kitchen sinks. The deep drawing process requires a blank, blank holder, punch, and die as shown in Fig. 1.2.

The blank is a piece of sheet metal, typically a disc or rectangle, which is pre-cut from stock material and will be formed into the part. The blank is clamped down by the blank holder over the die, which has a cavity in the external shape of the part. A tool called a punch moves downward into the blank and draws, or stretches, the material into the die cavity. The movement of the punch is usually hydraulically powered to apply enough force to the blank. Both the die and punch experience wear from the forces applied to the sheet metal and are therefore made from tool steel or carbon steel. The process of drawing the part sometimes occurs in a series of operations, called draw reductions. In each step, a punch forces the part into a different die, stretching the part to a greater depth each time. After a part is completely drawn, the punch and blank holder can be raised and the part removed from the die. The portion of the sheet metal that was clamped under the blank holder may form a flange around the part that can be trimmed off.

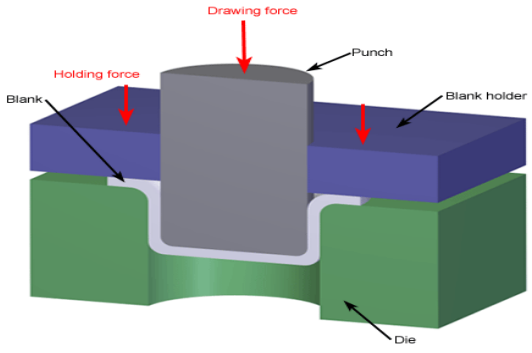

Fig. 1.2 Deep Drawing process (CustomPartNet, 2009)

1.3.3 Stretch forming

Stretch forming is a metal forming process in which a piece of sheet metal is stretched and bent simultaneously over a die in order to form large contoured parts. Stretch forming is performed on a stretch press, in which a piece of sheet metal is securely gripped along its edges by gripping jaws. The gripping jaws are each attached to a carriage that is pulled by pneumatic or hydraulic force to stretch the sheet. The tooling used in this process is a stretch form block, called a form die, which is a solid contoured piece against which the sheet metal will be pressed. The most common stretch presses are oriented vertically, in which the form die rests on a press table that can be raised into the sheet by a hydraulic ram. As the form die is driven into the sheet, which is gripped tightly at its edges, the tensile forces increase and the sheet plastically deforms into a new shape. Horizontal stretch presses mount the form die sideways on a stationary press table, while the gripping jaws pull the sheet horizontally around the form die.

Stretch formed parts are typically large and possess large radius bends. The shapes that can be produced vary from a simple curved surface to complex non-uniform cross sections. Stretch forming is capable of shaping parts with very high accuracy and smooth surfaces. Ductile materials are preferable, the most commonly used being aluminum, steel, and titanium. Typical stretch formed parts are large curved panels such as door panels in cars or wing panels on aircraft. Other stretch formed parts can be found in window frames and enclosures.

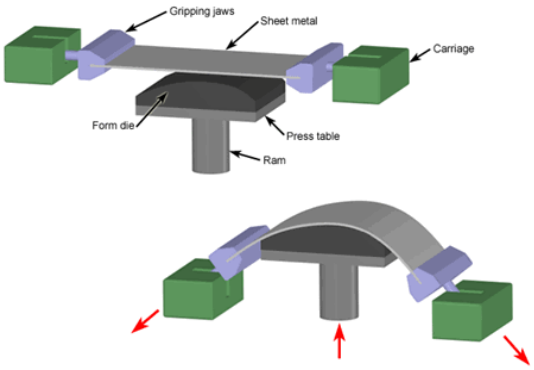

Fig 1.3 Stretch Forming process (CustomPartNet, 2009)

1.3.4 Ironing

Ironing of sheet metal is a manufacturing process that is mostly used to achieve a uniform wall thickness in deep drawings. Variation in wall thickness often exists in parts produced by deep drawing, as discussed in the previous section. Ironing of sheet metal can be incorporated into a deep drawing process or can be performed separately. A punch and die pushes the part through a clearance that will act to reduce the entire wall thickness to a certain value. While reducing the entire wall thickness, ironing will cause the part to lengthen. The percentage reduction in thickness for an ironing operation is usually 40% to 60%. Beverage cans are a common product of sheet metal ironing operations.

1.3.5 Bending

Bending is a metal forming process in which a force is applied to a piece of sheet metal, causing it to bend at an angle and form the desired shape. A bending operation causes deformation along one axis, but a sequence of several different operations can be performed to create a complex part. When bending a piece of sheet metal, the residual stresses in the material will cause the sheet to springback slightly after the bending operation. Due to this elastic recovery, it is necessary to over-bend the sheet a precise amount to achieve the desired bend radius and bend angle. The final bend radius will be greater than initially formed and the final bend angle will be smaller.

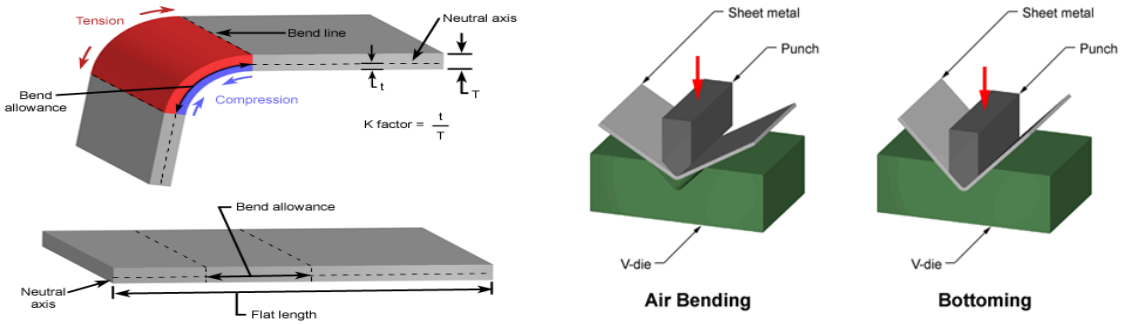

(a) (b)

Fig. 1.4 (a) Bending process (b) V-Bending Process (CustomPartNet, 2009)

The act of bending results in both tension and compression in the sheet metal. The outside portion of the sheet will undergo tension, while the inside portion experiences compression. The neutral axis is the boundary line inside the sheet metal, along which no tension or compression forces are present. As a result, the length of this axis remains constant.

The most common method is known as V-bending, in which the punch and die are "V" shaped. The punch pushes the sheet into the "V" shaped groove in the V-die, causing it to bend. If the punch does not force the sheet to the bottom of the die cavity, leaving space or air underneath, it is called "air bending". As a result, the V-groove must have a sharper angle than the angle being formed in the sheet. If the punch forces the sheet to the bottom of the die cavity, it is called "bottoming". This technique allows for more control over the angle because there is less springback.

1.3.6 Spinning

Metal spinning is a metal working process by which a disc or tube of metal is rotated at high speed and formed into an axially symmetric part. Spinning can be performed by hand or by a CNC lathe as shown in Fig.1.5. Metal spinning does not involve removal of material, as in conventional wood or metal turning, but forming or moulding of sheet material over an existing shape. Spinning process has low tooling cost and high production cost. Products have good surface finish. But the disadvantage of this process is that only axially symmetric components can be produced.

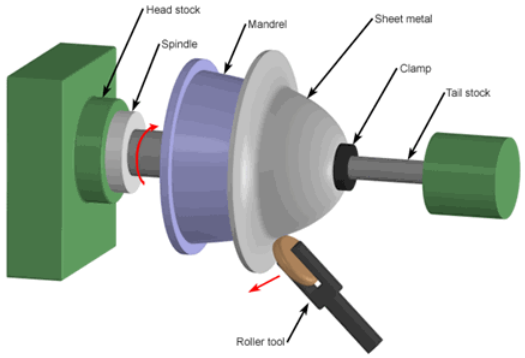

Fig. 1.5 Spinning Lathe (CustomPartNet, 2009)

1.3.7 Rubber forming

This process uses a flexible material, such as rubber or polyurethane, to form a sheet metal work piece. Often the rubber is incased in a steel container and serves as a punch. A work piece is placed over a rigid die. The punch forces the work into the rubber. Rubber is forced all around the work, creating pressure and forming the metal onto the die. This is known as the Guerin process. The location of the rubber can be switched between punch and die. In this case, a rigid punch presses a sheet metal work stock that is located over a die consisting of rubber incased in a steel container. The later process is illustrated in Fig. 1.6.

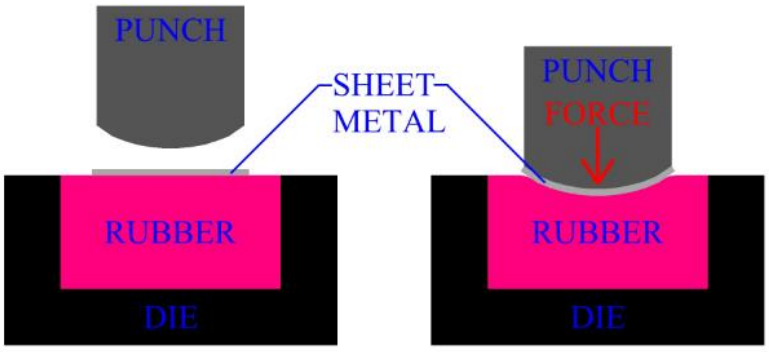

Fig. 1.6 Rubber forming (thelibraryofmanufacturing)

Rubber forming processes are limited in the depth of parts they can produce. Limitations in manufacturing exist because the pressure generated by the rubber is low, only 1500 lbs/in2, (10MPa). Rubber forming is used in the aircraft industry to produce sheet metal components. Low cost tooling makes setup for rubber forming inexpensive.

1.3.8 Hydroforming of sheet metal

Hydroforming is an effective sheet metal forming process. Hydroforming can typically obtain deeper draws than conventional deep drawing operations. Hydroforming uses a rigid punch to push a sheet metal work piece into a rubber membrane. Behind the rubber membrane is a chamber of pressurized fluid. When the work is pressed into the chamber, the rubber membrane surrounds it completely and the pressure of the fluid forces the sheet metal to form on the punch.

Fluid pressure can be controlled during the operation and can be as high as 15,000 lbs/in2, (100MPa). Due to the large amount of evenly distributed pressure on the work piece, very deep

draws, (high percent reduction), can be performed with hydroforming. Friction acts to reduce tensile stresses in the material during the process.

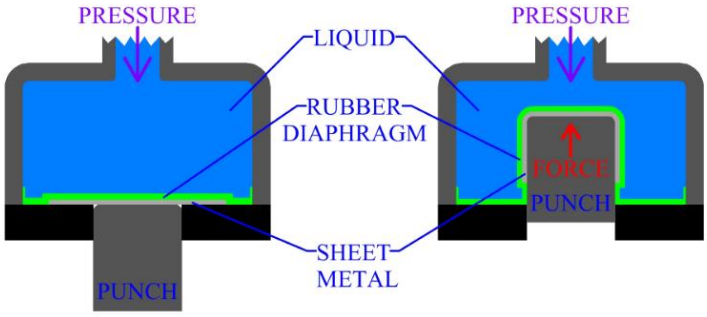

Fig. 1.7 Hydroforming of sheet metal (thelibraryofmanufacturing)

CHAPTER - 2
LITERATURE REVIEW

2.1 Characterisation of Sheet metals

Characterisation of sheet metal means the determination of various physical properties of sheet metal through experimentation. Mechanical testing plays an important role in evaluating fundamental properties of sheet materials as well as in developing new materials and in controlling the quality of materials for use in design and construction. If a sheet metal is to be formed in a predetermined shape for particular application, that will be subjected to a considerable deformation, it is important to know that the material is strong enough and rigid enough to withstand the load and deformation that it will experience in service. Some of prominent characterization tests that are performed are tensile test, peel test and anisotropy test. In the following section we will see the various research work done in this sphere.

2.2 Experimental evaluation for characterisation of sheet metal

2.2.1 Tensile test

The most common type of test used to measure the mechanical properties of a sheet metal is the Tension Test. Tension test is widely used to provide a basic design information on the strength of materials and is an acceptance test for the specification of materials. The major parameters that describe the stress-strain curve obtained during the tension test are the tensile strength (UTS), yield strength or yield point (σ_y), elastic modulus (E), percent elongation ($\Delta L\%$) and the reduction in area (r%), toughness, resilience, poisson's ratio(ν) can also be found by the use of this testing technique.

The tensile test for sheet metal is performed according to the ASTM standards. Akramifard H.R. et al (H.R. Akramifard, 2014) investigated the mechanical properties of cold roll bonded AA1050/AISI304 clad sheet. To estimate the mechanical properties of the Al-clad stainless steel sheets, they performed tension tests at room temperature using an Instron universal materials testing machine. Fig. 2.1 shows the details of the used tensile test specimen, which is in accordance with the subsize ASTM E-8 standard.

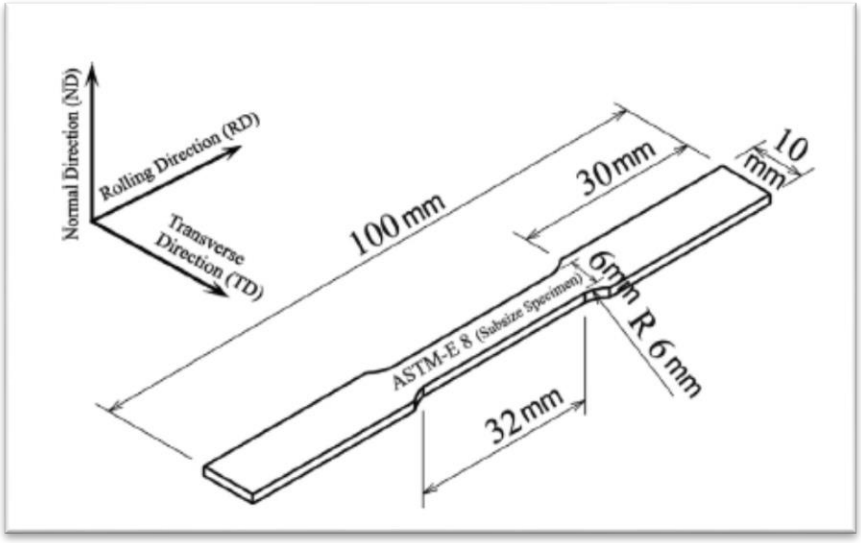

Fig. 2.1 Tensile test specimens (subsize ASTM E-8 standard) (H.R. Akramifard, 2014)

The results showed a significant drop in flow stress after the maximum point of the stress–strain curves (UTS) corresponding to the debonding of the interface. The UTS values were much lower than the tensile strength of the parent material 304L stainless steel (722 MPa) but was found out to be significantly higher than that of the annealed Al (72 MPa). The tensile strengths were found to decrease by increasing the post-anneal temperature. To discuss the mentioned trend, three different effects were considered: (1)the restoration processes during annealing treatment, (2)enhancement in the bond quality by post-heat treatment, and (3) the formation of inter-metallic compounds at the interface (in some cases). It seemed that the fracturing of the localized bonds during the tensile test occurs and exerts an influence on the tensile behavior. The drop after the maximum point of the stress–strain curves signified the effect of bond strength on tensile behavior and implied the fracturing of the localized bonds.

The tensile properties can also be determined using the rule of mixtures (Shi-Hoon Choi, 1997). The flow stress of (STS304/Al/STS304) sandwich sheet is found to follow the rule of mixtures law according to the following equation :

$$\sigma_{uS} = \sigma_{uA}.V_A + \sigma_{uB}.V_B \quad (1)$$

where σ and V are uniaxial flow stress and volume fraction and subscripts S, A and B stands for sandwich material and components A and B layers respectively. Fig. 2.2 shows the flow curves obtained from the rule of mixtures compared with the measured one. The flow stresses calculated

using rule of mixtures are practically equivalent to the measured flow stresses.

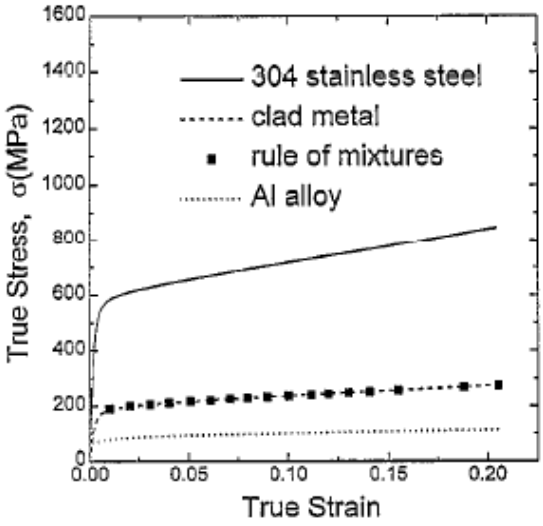

Fig. 2.2 Tensile curves of STS304-clad aluminum bilayer sheet and its components (Shi-Hoon Choi, 1997).

2.2.2 Peeling test

Peeling test is conducted to check the bond strength that the clad sheet can withstand under loading conditions. To ensure the bond strength of Al-clad stainless steel sheets, the roll bonding process was performed in various reductions in thickness (Akramifard H.R. et al., 2014). Peeling test specimens were prepared from the clad sheets according to ASTM-D1876-01 standard as shown schematically in Fig. 2.3

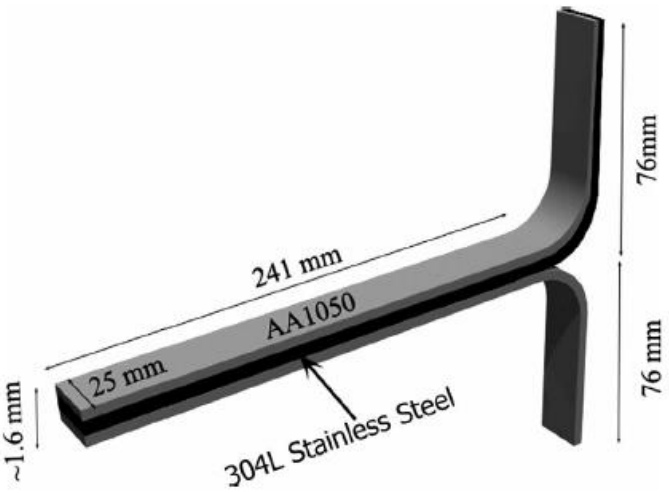

Fig 2.3 Peel test specimen according to ASTM-D1876-01 standard (H.R. Akramifard, 2014)

The average peel strengths (σ_{Peel}) were determined using the equation σ_{Peel}=F/W, where F is the average load of the fluctuating portion of the peeling force diagram and W is the bond width. Various samples were prepared with reduction in thickness from 10% to 38% at room temperature. The peel strength was found to increase from 3 N/mm to 20N/mm in the above mentioned thickness range. The observed tearing of the AA1050 sheet of roll-bonded sheet during the peel test after roll bonding by 38% reduction without post-heat treatment implies that the bond strength of the clad sheet has reached the strength of AA1050.

2.1 Formability of Sheet metals

Formability is the ability of a given sheet metal to undergo plastic deformation without being damaged. The plastic deformation capacity of metallic materials is limited to a certain extent, at which point, the material could experience fracture or tearing. Knowledge of the material formability is very important for the design and layout of any industrial forming process. Simulations using the finite-element method and use of formability criteria such as the forming limit curve (forming limit diagram) enhance and, in some cases, are indispensable to certain tool design processes

2.2 Experimental evaluation for Formability of sheet metal

Akramifard et al. (H.R. Akramifard, 2014) carried out experimental studies on effect of percentage-reduction by rolling and subsequent annealing temperatures on mechanical properties and bond strength of three layered AA1050-304L-AA1050 clad sheets, during roll bonding. A significant drop in tensile stress–strain curves after the maximum point (UTS) was correlated to the interface de-bonding. It was found that the formation of intermediate layer by post heat treatment deteriorates the bond quality and encourages the de-bonding process. Moreover, the existence of strain induced martensite in clad sheets was found to play a key role in the enhancement of tensile strength. Choi et al. (Shi-Hoon Choi, 1997)experimentally investigated the deformation behaviour of Al-STS430 bi-layer clad sheets under uniaxial tension and concluded that a difference in planar and normal anisotropy results in the warping of edges of tensile specimens. Masoumi and Emadoddin (Masoumi, 2013) carried out the research work on formability and bond strength between two and three-layered Al/SiCP sheets manufactured by the roll bond process at different thickness reductions and different number of layers by Erichsen cupping test and lap–shear test. Yoshida and Hino (Yoshida, 1997) investigated the formability

of two and three ply steel-aluminium clad sheets. It was observed that in the analytical predictions and the experimental observations, the FLDs of the laminates lie between those of their component sheet metals. The effect of prestrain generated in the roll-bonding process on the formability was also discussed. Lee and Kim (Lee, 1988) investigated the application of rule of mixtures to predict the flow stress in stainless steel-aluminium-stainless steel sandwich sheets. The calculated values were in good agreement with the measured data, though Hosford's yield criterion and Hill's new yield criterion yielded slightly better results than Hill's quadratic yield criterion for anisotropic materials.

There are many tests of formability for sheet materials. A given test may correlate well with behavior in one type of forming process and poorly with behavior in another. This is because the relative amounts of drawing and stretching vary from test to test and process to process. Swift Cup test, LDH Test are the different tests which were used to assess the formability of sheet-metal.

2.2.1 Limiting dome height (LDH) test

The Limiting Dome Height test is a formability test designed for the sheet metal industry. It tests the material in or near planestrain. Under properly controlled conditions, it appears to be as stableas other classic material tests. The simplicity of the procedure and its simulative nature make it a good test for the statistical monitoring of incoming material in a stamping production environment.

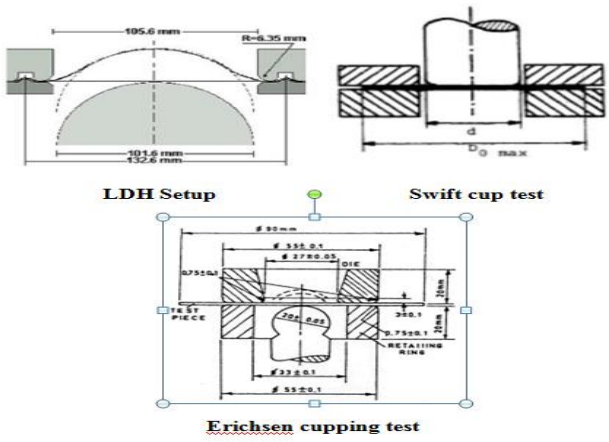

Fig. 2.4 Formability tests (H. Danesh Manesh, 2003)

Being a simulative test, it integrates the effects of parameters such as work hardening, ductility and friction into a single numerical value, the LDH value.

In this test, rectangular blanks of varying widths are clamped firmly in the longer direction and stretched over a hemispherical punch, thereby varying the transverse constraint to control the amount of lateral drawing-in.

2.2.2 Swift Cup Test

Another common method to test sheet formability is the swift cupping test. The Swift-cup test is a drawing test. A series of blanks with steadily increasing diameters are deep drawn, and at one point a diameter is reached, where the punch penetrates the not yet completely drawn cup. The Swift cup test is the determination of the limiting drawing ratio for flat-bottom cups.A simulative test in which circular blanks of various diameter are clamped in a die ring and deep drawn into a cup by a flat-bottomed cylindrical punch.

The Swift Cup test is usually considered to provide a measure of the drawability of sheet metal. A schematic representation in Swift Cup test is shown in Figure 3. A disc-shaped sheet specimen of metal is placed between the blank holder and the die and then it is drawn into a cup by a cylindrical punch. A cup with a cylindrical shape will be form after the test. A high Swift number indicates a good drawability and vice-versa.

2.2.3 Erichsen cupping test

The Erichsen tests (Dieter, 1988)are used to estimate sheet metal formability under pure stretching conditions. The sheet is clamped between two flat plates and is stretched by a ball. The height of the cup represents the formability index. Cups with larger height represent good resistance to necking. The Erichsen test produce bending strains in the test and hence no longer used in the industry.

2.2.4 Forming Limit Diagram

The first forming limit diagram was published by Keeler (Keeler, 1961). But he determined the forming limit curve only in the positive range of minor strain (i.e. for $\varepsilon 2 > 0$). The left hand side (i.e. for $\varepsilon 2 < 0$) was then determined by Goodwin (Goodwin, 1968) and since then it is called as the Keeler-Goodwin diagram. This type of forming limit diagram is shown in Fig. 2.5. The curve connecting the fracture points of each strain paths is called forming limit curve and denoted by

FLC. For most materials in conventional forming processes, the forming limit diagram has a typical V shaped form as seen in Fig. 2.5. Various strain paths shown in the below figure is (1-pure shear, 2-uniaxial tension; 3-plain strain; 4, 5 6-different biaxial tension) (Miklós Tisza, 2012)

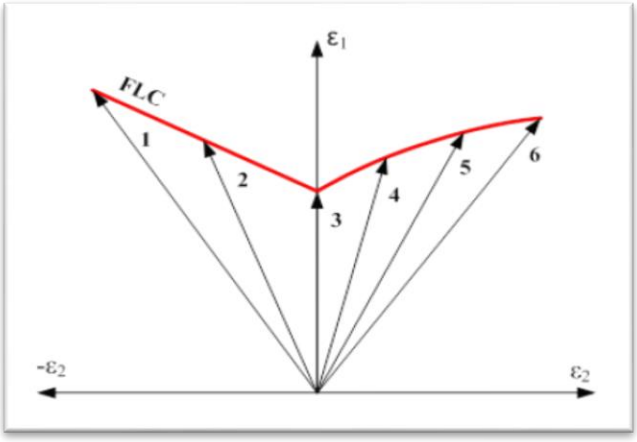

Fig. 2.5 Forming Limit Diagram for various strain paths

2.2.5 Basic understandings concerning the forming limit diagrams

Forming Limit Diagrams represent the formability limits in the coordinate system of major (ε1) and minor (ε2) principal strains as shown in Fig.2.5. The formability limit is usually characterized by the failure (rupture) and this is called as formability (fracture) limit curve . However, it is evident that in normal production conditions even the local necking cannot be permitted: neither from the point of view of aesthetic appearance nor the functional operation of the part. This is the reason that further limit curves are determined besides the rupture for the limit of necking as well. The zone between the fracture and the necking limit curve is called as the range of local necking. At certain level of compressive stresses a local instability of sheet can also occur: this phenomenon is regarded as wrinkling. It is also evident that besides rupture and local necking, wrinkling should also be avoided. The forming limit diagram with these limit curves and zones is shown in Fig.2.6. Below the local necking zone, the green zone indicates the safe region of normal forming conditions in terms of major (ε1) and minor (ε2) principal strains.

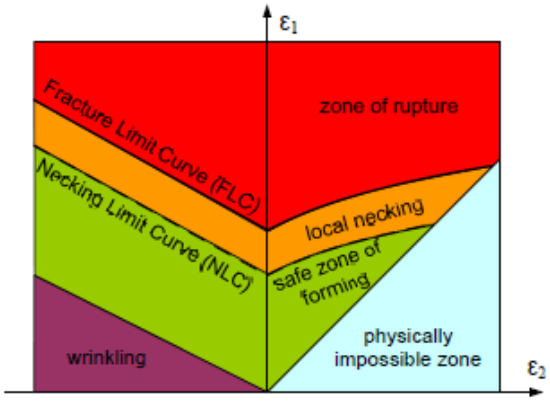

Fig. 2.6 Various zones in FLD (Miklós Tisza, 2012)

As it can be seen from the Fig. 2.6, there are various limit curves and also the zones denoted by different colours mean different behaviour from the point of view of formability. The Fracture Limit Curve which is more often called as Forming Limit Curve (FLC) represents those limit values of ε1 and ε2 where fracture occurs. While to observe the onset of fracture is quite easy, however to determine the principal strain values at the onset of rupture is rather complicated.

The Necking Limit Curve (NLC) represents the onset of local necking. Though the exact measurement of principal strain components at the limit state of necking is at least as difficult as it is for the onset of fracture, but this limit is more acceptable for real industrial parts, since at this stage still there is no any undesirable local necking.

2.2.6 Analysis of parameters affecting the Forming Limit Diagrams

The determination of forming limit diagrams is a quite complicated process and during their determination we have to consider many parameters that may influence it. The most important influencing parameters are (Miklós Tisza, 2012):

- the strain path, i.e. the strain history applied during the investigations,
- the material quality and the various material properties (e.g. the strain hardening coefficient (n), the strain-rate sensitivity index (m), the anisotropy coefficient (r), the rolling direction, etc.)
- the sheet thickness (t),
- the shape and sizes of specimens,

- the experimental conditions (e.g. the shape and precision of applied grid, the precision of grid measurement, the temperature, the friction conditions, etc.)

CHAPTER - 3
MOTIVATION AND OBJECTIVES

From the discussion from previous section we observe lot of study is focused now-a-days on clad metal sheet of different grades and thickness. With the increase in application of clad sheets in various industries like cookwares, automobile industry, a large number of FE simulations are being carried out to simulate the sheet metal forming operations like stretching, deep drawing, bending etc. Accuracy of failure prediction in FE simulations of clad sheet depends on the influence of sheet thickness and mechanical properties of the individual sheets. Mechanical properties of the sheet in turn depend on grade (type of alloy content and composition) and the conditions (heat treatment after cold rolling).

In view of this, it has been planned to study a such clad sheet formed of cold roll bonding and after heat treated. This study is confined the AISI304/AA1050/AISI430 clad sheet with combined thickness of 2.5mm.

3.1 Objectives

The specific objectives of the work are identified as:

1) Characterization of tensile properties and forming parameters of the clad sheet and individual components and their comparision.
2) To determine the Peel strength of the roll bonded clad sheets
3) To determine the drawability by evaluating the Normal anisotropy.
4) Experimental determination of forming limit diagram(FLD) for the clad sheet metal.
5) To compare the FLD_o obtained from the experimental and Keeler Godwin equation.
6) Failure pediction in Limit Dome height test through Finite Element analysis
7) Comparing the Experimental result with the simulation result.

CHAPTER - 4
METHODOLOGY

The methodology is explained here under sections i.e. experimental work and Finite element analysis.

4.1 Experimental work

The details of experimental work carried out for determining the tensile properties, peel test, anisotropy test, formability parameters, limited dome height and forming limit strains of try ply AISI304/AA1050/AISI430 clad sheet are explained in this section.

4.1.1 Selection of materials

The present study has been carried out on tri-ply clad sheet, containing AISI304L austenitic stainless steel on one side and AISI430 on the other side with AA1050 in the core of the blank, with a combined thickness of 2.5mm.

Circular blanks of tri-ply clad sheet of AISI304/AA1050/AISI430 material of effective thickness of 0.4, 1.5 and 0.6mm respectively, that are joined by roll bonding and thermal treatment, due to a metallurgical bond under high pressure, was procured from a leading supplier in India.

4.1.2 Chemical composition of clad sheet materials

The chemical composition of individual sheets were obtained by spectrometry- analysis and are given in Table 4.1.

Table 4.1 Chemical compositions of sheet materials used in the clad sheet

Sheet material	C	Mn	Si	Al	Ni	Cr	S	P
AISI304	0.057	1.45	0.82	0.044	9.62	18.034	0.009	0.023
AISI430	0.12	0.902	0.675	0.038	0.621	17.02	0.023	0.026
AA1050	0.18	0.018	0.156	Rest	0.032	0.012	0.015	0.034

4.1.3 Peeling Test

To investigate the bond strength due to cold roll bonding (CRB), the peeling test was performed according to ASTM-D1876-08 standard (subsized). Specimens for the peel test were laser cut in the sub-size of 160X 25 mm due to limited availability of the material. Since it is difficult to detach the bonded sheets mechanically, one end of the each specimen was immersed in the solution of sodium hydroxide to dissolve aluminium. The remaining length with intact bond was used for the peel test as shown in the Fig. 4.1. The specimens were prepared in such a way that each bonded sheet of steel i.e. AISI304 and 430 be peeled from aluminium bond respectively. The stainless steel sheet to be peeled was held in the lower fixed jaw and the rest with the upper movable jaw fixed with the cross -head on the 50kN UTM. All the tests were conducted at a cross head speed of 10mm/min.

Fig. 4.1 Peel test arrangement on 50kN UTM

4.1.4 The Tensile test

Most common approach to characterize the behaviour of a material is by conducting uniaxial tensile tests. In this work, simple tension tests were carried out on a universal testing machine of maximum capacity 50 kN as shown in Fig. 4.5. The tensile test specimens as per ASTM-E8M shown in Fig. 4.2 were prepared by laser cutting of the blank as shown in Fig. 4.3. The tests were carried out at a cross head speed of 2.5mm/min. Typical engineering stress strain curve is plotted on the basis of force and displacement data acquired from the dedicated software.

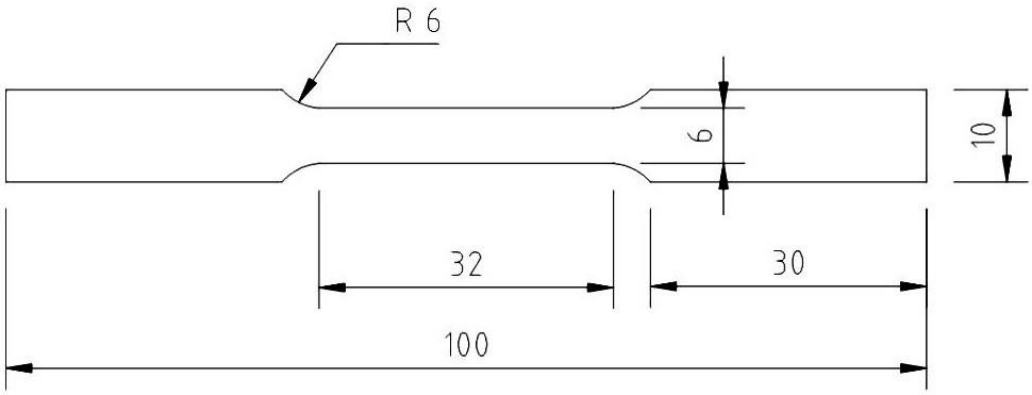

Fig. 4.2 Dimensions of Tensile specimen (mm) (ASTM E8)

4.1.4.1 Tensile test for Clad sheet

The tensile test of the tri-ply clad sheet metal was investigated by performing tensile tests at specimen orientation of 0°, 45° and 90° to the rolling direction (RD) and are shown in Fig. 4.4. Each test is performed at least three times to ensure good reproducibility of the experiments.

Fig. 4.3 Laser cutting of tensile specimens

4.1.4.2 Tensile test for Individual components of the clad sheet

Individual components were collected by dipping the clad sheet specimen in sodium hydroxide solution for a month . The aluminum was dissolved remaining left with the AISI304 and AISI430. The procedure was done for three samples each for specimens oriented at 0°, 45° and 90° to the rolling direction (RD).

Fig. 4.4 Tensile specimens at different orientations (Before And After the test)

The strain hardening exponent (n) and the strength co efficient (K) values are calculated from the stress strain data in uniform elongation region of the stress strain curve. The plot of ln(True stress) versus ln(True strain) which is a straight line is plotted as discussed below :

The power law of strain hardening is given as :

$$\sigma = K \epsilon^n \qquad (4.1)$$

where σ and Є are the true stress and the true strain respectively.

Taking log on both sides

$$\text{Log}(\sigma) = \log(K) + n \log(\epsilon) \qquad (4.2)$$

This is an equation of straight line and the slope of which gives the value of 'n' and 'K' can be calculated taking the inverse natural log of the y intercept of the line.

For determining the n value of these sheets, the engineering stress strain data were converted into true stress-true strain curves using the following equations.

$$\sigma = s(1 + e) \qquad (4.3)$$

$$\varepsilon = \ln(1 + e) \qquad (4.4)$$

Where s = engineering stress and e= engineering strain.

4.1.5 Determination of average plastic strain ratio (Normal anisotropy – R_{avg} value)

The anisotropy test specimens as per ASTM-E8M were prepared by laser cutting of the blank as shown in Fig. 4.3. The anisotropy of the tri-ply clad sheet metal was investigated by performing tensile tests at specimen orientation of 0°, 45° and 90° to the rolling direction (RD) each three times and are shown in Fig. 4.4. The tests were carried out at a cross head speed of 2.5mm/min.

Fig. 4.5 50kN Universal testing machine

The specimens were elongated to predetermined longitudinal strain (20%)and the testing was stopped before the onset of necking. Final width and gauge length were measured and the plastic strain ratio (R) is calculated as below [George E Dieter, Mechanical metallurgy]:

$$R = \frac{\varepsilon_w}{\varepsilon_t} = \frac{\varepsilon_w}{-(\varepsilon_w+\varepsilon_l)} \quad (4.5)$$

$$\varepsilon_w = \ln\frac{w_f}{w_0} \quad (4.6)$$

$$\varepsilon_l = \ln\frac{l_f}{l_0} \quad (4.7)$$

W_0, l_0: initial width and length, W_f, l_f: final width and length

ε_w=true width strain

ε_t=true thickness strain

ε_l=true length strain

The R value was determined in three directions by repeating the above procedure. The normal anisotropy or average plastic strain ratio was calculated using the formula:

$$\mathbf{R_{avg} = (R_0 + R_{90} + 2R_{45})/4}$$

R_0, R_{45} and R_{90} represent the R value in three directions.

4.1.6 Limit Dome height test (LDH)

As suggested by Hecker [1974], samples of varying width were deformed using a hemispherical punch with 50 mm diameter. The dog boned shaped sample widths were varied to obtain all possible deformation modes i.e. biaxial tension, plane strain tension and tension-compression. The sample widths taken into for LDH were 20mm, 30mm, 40mm, 50mm, 60mm, 70mm, 80mm and 100mm. The schematic diagram of the arrangements of tools used in experiments is shown in Fig. 4.6

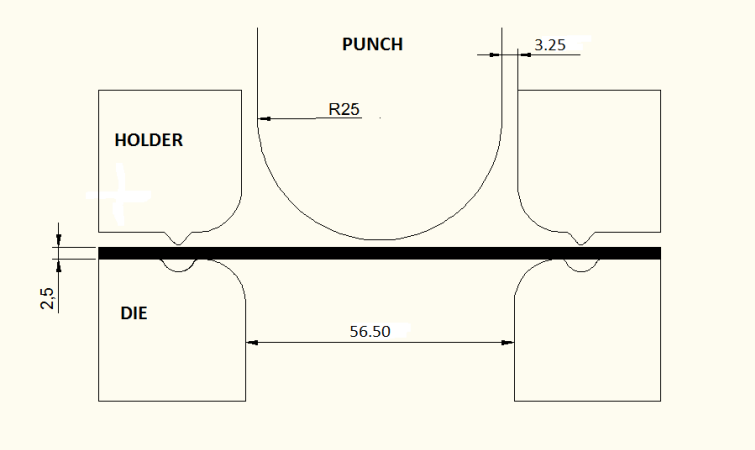

Fig. 4.6 Schematic diagram of punch and die setup for LDH tests

A 50 mm diameter punch was used with dies (lower die and blank holder) having a draw bead to prevent the drawing in of the blank for certain widths. The draw bead ensures that only portion of blank within the die region is stretched completely without drawing. The sheet strips of varying widths were clamped firmly between the die and the blank holder before they were stretched over the punch. The extent of drawing in during punch stretching depends on the width of the blank. As the width decreases the drawing component increases and stretching component decreases. In the current setup the draw bead diameter is 84 mm. So samples of widths 50,60,70,80 and 100 mm as shown in Fig.4.8 were used to get data in biaxial tension region.

Samples having width varying from 20mm to 40mm were used for strain data with negative minor strain. Three samples were used for each width to ensure good reproducibility of the experiments. The blanks were laser marked with 2.5mm diameter circles with a gap of 0.5 mm between the circles as shown in Fig. 4.7. Samples of 60mm width were found to give zero minor strains (plane strain condition).

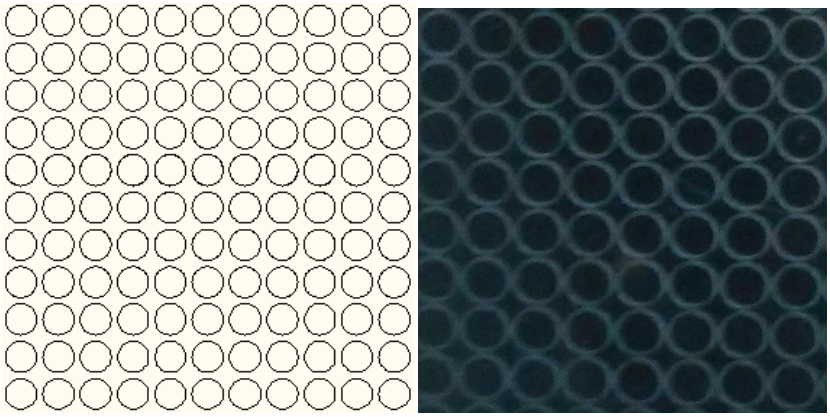

(a) (b)

Fig. 4.7 (a)Pattern of grid marking on the specimen and (b) Grid marked specimen (on AISI430 surface)

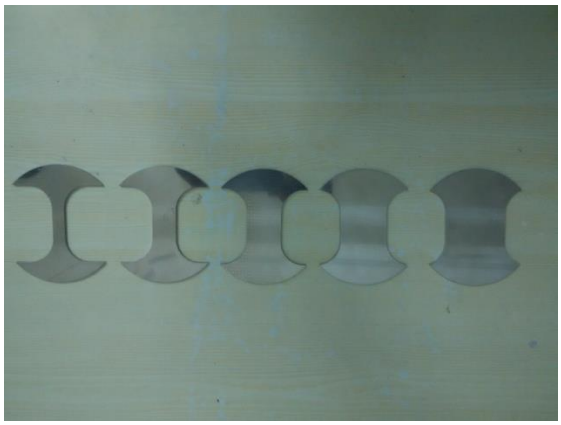

Fig. 4.8 Specimens before LDH test

4.1.6.1 Tool Design

The design of the die, blank holder, draw bead and punch plays prominent role on the quality of the final product. Important parameters must be kept under consideration while tool design. The following section discusses about the designing of the above mentioned tools.

The 50mm diameter hemispherical punch is used, so the die and blank holder inner diameter is 56.5 mm taking the clearance in consideration which is 3.25 mm. The outer diameter of both die and blank holder is 100 mm. The punch, die and blank holder were fabricated through CNC milling using AISI D2 Tool steel material and air hardened upto 60 HRc. The chemical composition of the tool material is observed by spectrometry analysis and is given in Table 4.2.

Table 4.2 Chemical composition of AISI D2 tool steel material

Material	C	P	Mn	Si	S	Ni	Cr	Mo	Cu	Al	Sn
AISI D2 Tool steel	1.64	0.014	0.4	0.29	0.003	0.23	11.4	0.73	0.14	0.029	0.004

The circular draw beads were designed on die and blank holder with a diameter of 84 mm. The entrance and groove radius of draw bead is 1 mm. the entrance and groove angle is 55^0. The depth and width of the draw bead is 2.8 mm and 6 mm respectively. Fig 4.9 shows the CAD drawing of the die, holder and drawbead.

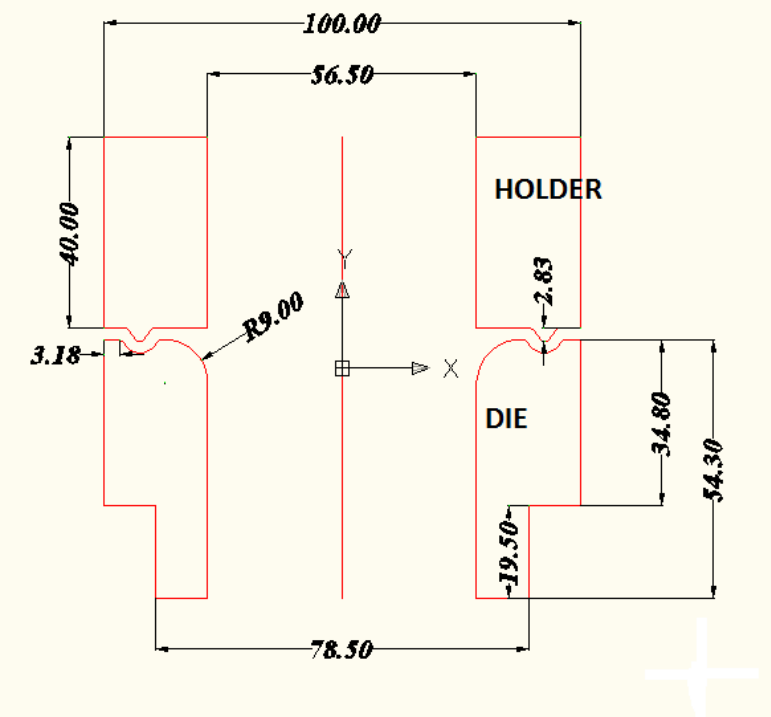

Fig.4.9 Die, holder and draw bead design in CAD

4.1.6.2 Limit Dome Height experiment

The grid marked specimens were deformed using a double action hydraulic press of 100-tonne capacity. A view of the experimental setup mounted on the hydraulic press is shown in Fig. 4.10.

Fig. 4.10 Experimental setup on 100-tonne Hydraulic press

The specimen was placed between the upper and the lower dies as shown in Fig.4.11. An optimum blank holding force in the range of 1-1.5 tonnes was applied manually on the upper die to clamp the blank at the draw bead. The experiment was stopped when a visible neck or initiation of fracture was obtained on the specimen. In all the above stretch forming experiments a data acquisition system consisting of a load cell and a rotary encoder was used to obtain the load - displacement data during the experiments. Amplifier was used to amplify the signals from the load cell and the rotary encoder. These amplified signals are converted to digital signals by analog to digital converter and fed to the computer. From these digital data, a load - displacement curves were plotted.

Fig. 4.11 Arrangement of Die-Holder-Punch-Blank on hydraulic Press bed

4.1.6.3 Strain measurement

Major and minor principal strains were calculated by measuring major and minor diameters of ellipses on the deformed samples. A Stereo zoom travelling microscope having a least count of 0.001mm was used to measure major and minor diameters of ellipses for strain calculations. A picture of stereo zoom travelling microscope taking measurement is shown in Fig. 4.12. The dedicated software takes photographs and measurement of the images taken by the microscope. Fig. 4.13 shows the measurement which is taken by the software.

Fig. 4.12 Stereo zoom Travelling Microscope

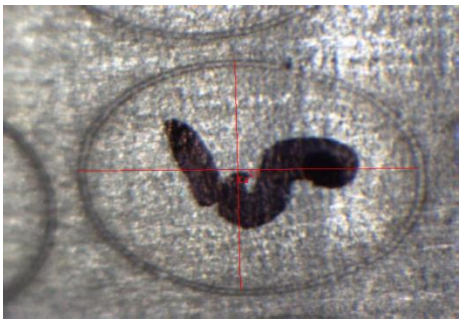

Fig. 4.13 Measurement of a ellipse taken by travelling microscope

4.1.6.4 Height measurement

The limit dome height (LDH) of all the specimens at the point of necking/fracture was measured using a vernier height gauge with a least count of 0.02 mm.

4.2 Finite Element Analysis (FEA)

The finite element analysis (FEA) is a numerical technique for finding approximate solutions to boundary value problems . It is also referred to as finite element method (FEM). FEA subdivides a large problem into smaller, simpler, parts, called finite elements. The simple equations that model these finite elements are then assembled into a larger system of equations that models the entire problem. This method is used for predicting how a product reacts to real-world forces, vibration and other physical effects. Finite element analysis shows whether a product will break, wear out, or work the way it was designed for.

In the present work, the finite element analysis was carried out for the prediction of failure in limit dome height test for AISI304/AA1050/AISI430 clad sheet . The FE simulation was carried out in ABAQUS/Explicit 6.10 to simulate the deformation behaviour of clad metal sheet.

4.2.1 FEA of Limit dome height test

The FE simulations were done to check to check the accuracy of failure prediction in LDH of AISI304/AA1050/AISI430 clad sheet with varying widths. The failure predictions of FEA were compared with the experimental results.

The LDH simulations were carried out using a 50 mm hemispherical diameter punch. In this case, a 1/2 symmetric model in 3D was created as shown in Fig. 4.14. The clad metal sheet was considered as an isotropic material with three different layers. The design parameters are given

in Table 4.3. The blank is a deformable solid body having the dimensions 2.5 mm in thickness, 55 mm in length and width was given by solid extruding the blank to the required value of width.

Table 4.3 Design parameters for FE analysis

Design parameter	Dimension(mm)
Die inner diameter	56.5
Die outer diameter	110
Holder outer diameter	110
Punch Diameter	50
Clearance	3.25
Die corner radius	9
Draw bead diameter	84
Blank thickness	2.5

The sheet thickness was cell partitioned into three parts into thickness of 0.4mm, 1.5mm and 0.6mm which is sectioned to three materials SS304, AA1050 and SS430 respectively. Various widths represents three different modes of deformation namely biaxial stretching, plain strain condition and tension-compression respectively.

4.2.2 Material Model

ABAQUS/Explicit 6.10 was used to simulate plastic deformation behaviour of blanks during LDH test. The material properties previously determined from tensile tests were used to simulate the actual flow rule of the clad metal sheet. The blank was meshed with 8 node linear brick elements (C3D8R) with reduced integration and hourglass control, whereas the die, punch and holder plate were considered to be discrete rigid bodies with 4-node, 3D bilinear rigid quadrilateral elements (R3D4). The 2.5 mm sheet was designed as deformable body extruded to various widths that was required for various simulations. The sheet was cell partitioned using reference datum planes. The material properties that were sectioned to three regions were taken from the results of the tensile test results of the individual sheets. The top surface was designated

with SS304, inner core as AA1050 and bottom region as SS430. The material properties that were given to the solver are given in Table 4.4.

Table 4.4: Material properties used in FE simulations

Material Grade	Thickness (mm)	Yield stress (MPa)	Tensile strength (MPa)	% elongation	Strain hardening exponent	Strength coefficient (MPa)
AISI304	0.4	155	381	57.6	0.45	686
AA1050	1.5	38	116	22.8	0.28	231
AISI430	0.6	310	427	30.3	0.42	1165

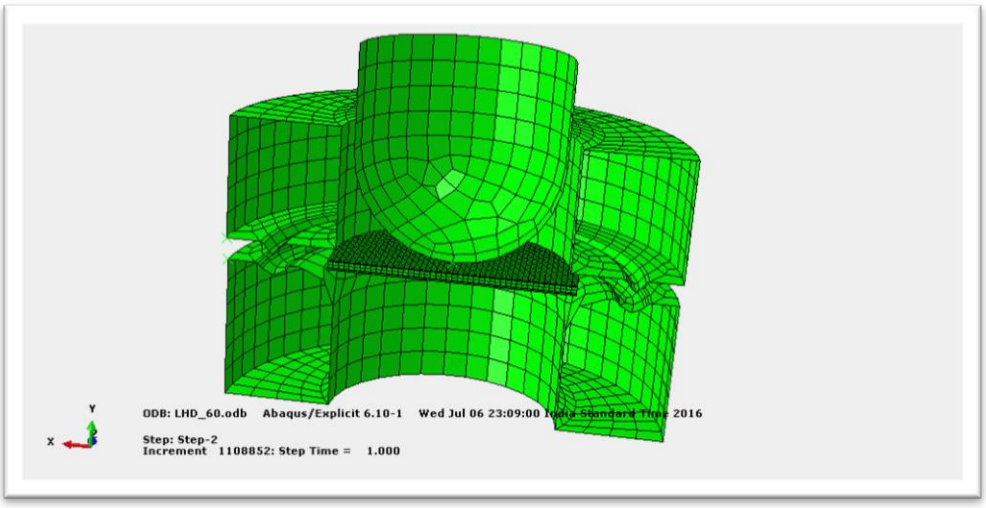

Fig. 4.14: Arrangement of tools and blank in FEA simulation in ABAQUS 6.10

4.2.3 Process Parameters

The punch was specified to move in the z-direction, and a holding force was applied on the blank through a blank holder. The draw bead was modelled to restrict the flow of material into the die. Three contact pairs i.e. punch–blank, holder–blank, and blank–die were defined in the simulations. The Coulomb coefficient of friction was set to 0.15 for holder-blank and die-blank interfaces, whereas a friction value of 0.05 was used for punch-blank interface. The clearance between the die and the punch was kept as 3.25mm. The process parameters used in Finite element analysis is given in Table 4.5

Table 4.5: Process parameters used in FE simulations

S.No.	Process Parameter		Value
1	Coefficient of friction between	Blank-Holder	0.15
		Blank-Die	0.15
		Blank-Punch	0.05
2	Blank Holding Force		1,90,000 N

The punch displacement provided is different for different widths and they are equal to the limit dome height observed from the experimental procedure. The data for punch displacement for each width is provided in Table 4.6

Table 4.6: Punch Displacement given in FE simulations

S.No.	Sample width (mm)	Dome height at necking (mm)
1	20	25.06
2	30	24.33
3	40	24.98
4	50	24.39
5	60	18.04
6	70	21.5
7	80	19.26
8	100	19.6

CHAPTER - 5
RESULTS AND DISCUSSION

5.1 Average peel strength

The bond/peel strength of AISI304 and AISI430 from the AA1050 sheet per unit length is shown in Fig. 5.1. The average peel strength is determined as the ratio of peeling force to the peeling width. The range of the peeling strength of AISI304 from aluminium is observed to be 30 to 51N/mm, whereas peeling strength of AISI430 from aluminium is found to be 20 to 26N/mm. The experimental investigation showed that the peeling strength of AISI 304 is higher than AISI 430 by a factor of 1.5 on average basis. In both the peeling tests, the peeling strength remained constant for an appreciable length of 80mm with a slight dip at a peeling distance of 190mm.

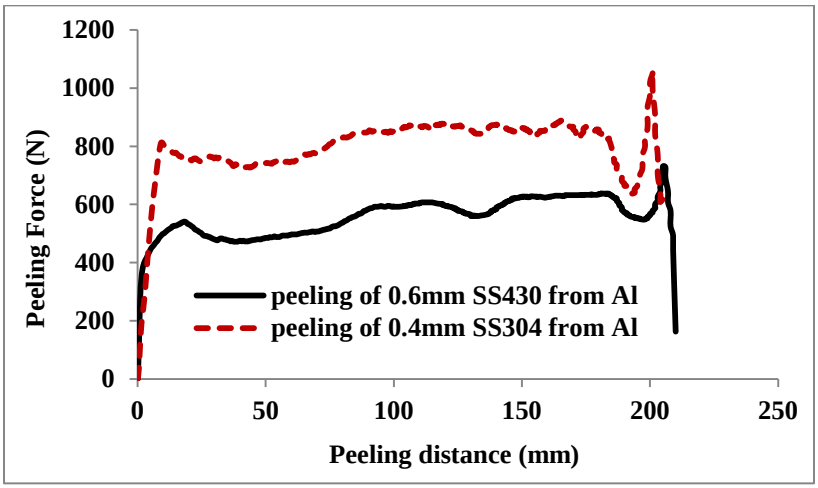

Fig. 5.1 Peeling force vs. distance curves for determination of bond strength

Near the end of the experiment the peeling strength is observed to increase which could be attributed to the shear deformation at the time of preparing samples. Same trend is observed in all the tests conducted.

5.2 Tensile properties

The average values of tensile properties obtained by uniaxial tensile tests of the samples of clad sheet are given in Table 5.1. The tensile strength of the clad sheet samples oriented at 90° w.r.t the rolling direction is highest and the ductility is lowest when compared with samples of other orientations. The measures of ductility are the n value (strain hardening exponent), uniform elongation, total elongation and the *R* value (Lankford value). The plastic strain ratio is observed

to be the lowest along the rolling direction and highest in the samples oriented at 45° w.r.t. the RD. The strain hardening exponent is approximately 0.25 which indicates appreciable uniform elongation or workability at room temperature. The normal anisotropy ($\bar{R}$) which also indicates a low resistance to thinning in deep drawing is found to be 0.78. The planar anisotropy of the clad sheet is very low (-0.06) which is good for minimizing earing defects during deep drawing process. The tested tensile samples are shown in Fig. 5.2. In all the samples, the crack initiated from the AISI 430 side of the specimens. This could be attributed to the lower ductility. A waviness pattern is also seen on edges of the samples due to difference in anisotropy of the individual sheets.

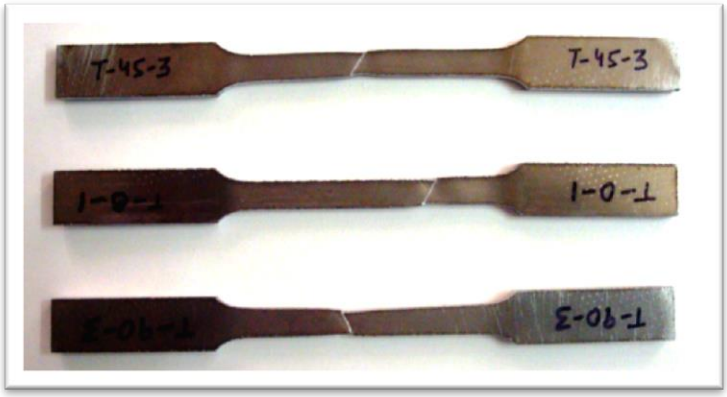

Fig. 5.2 Tested tensile samples

Table 5.1 Average tensile properties of clad sheet metal

Specimen's orientation w.r.t. RD	Yield stress (MPa)	Tensile strength (MPa)	% elongation	Strain hardening exponent	Strength coefficient (MPa)	Plastic strain ratio
0°	171	248	53.2	0.25	438	0.72
45°	177	249	51.0	0.26	465	0.81
90°	176	258	47.5	0.25	463	0.78

The deformation behaviour in uniaxial tension of individual sheets samples i.e. SS430, SS304 and AA1050 are also investigated and the average tensile properties are given in Tables 5.2, 5.3 and 5.4 respectively.

Table 5.2 Average tensile properties of SS430

Specimen's orientation w.r.t. RD	Yield stress (MPa)	Tensile strength (MPa)	% elongation	Strain hardening exponent	Strength coefficient (MPa)
0°	290	413	28.3	0.31	908
45°	310	427	30.3	0.42	1165
90°	302	421	24.2	0.48	1272

Table 5.3 Average tensile properties of SS304

Specimen's orientation w.r.t. RD	Yield stress (MPa)	Tensile strength (MPa)	% elongation	Strain hardening exponent	Strength coefficient (MPa)
0°	156	285	49.7	0.44	584
45°	155	381	57.6	0.45	686
90°	166	370	45.7	0.40	715

Table 5.4 Average tensile properties of AA1050

Specimen's orientation w.r.t. RD	Yield stress (MPa)	Tensile strength (MPa)	% elongation	Strain hardening exponent	Strength coefficient (MPa)
0°	38	116	22.8	0.28	231
45°	37	103	25.3	0.29	216
90°	36	106	23.4	0.32	234

It is observed that the tensile strength of SS430 is the highest than the rest of the sheets used in clad combination. The yield strength of the SS430 grade is twice the yield strength of AISI304 and approximately 7.8 times the yield strength of AA1050. Samples oriented at 45° to RD shows highest tensile strengths in both the cases of AISI430 and AISI304 followed by the samples

oriented at 90° and 0° w.r.t. RD. The ductility of AISI304 is the highest. The ductility of clad sheets is majorly contributed by the ductility of AISI304. This due to the fact that at the point of instability (UTS) delamination/ debonding starts followed by necking. The crack appeared first on AISI430 and then necking appears on AISI304. Interestingly, no crack was observed in the aluminium core of the tested tensile samples of clad sheet. The strength of the clad sheet may be equal to the average value which is based on the thickness ratio of the separate sheets. In making the clad sheets the temperature of the annealing is the hot working temperature for aluminum but the cold or warm working temperature for stainless steels. This may affect the properties of SS and aluminium in a different manner.

A comparison of true stress-true strain plot of clad sheet and individual sheets is shown in Fig. 5.3.

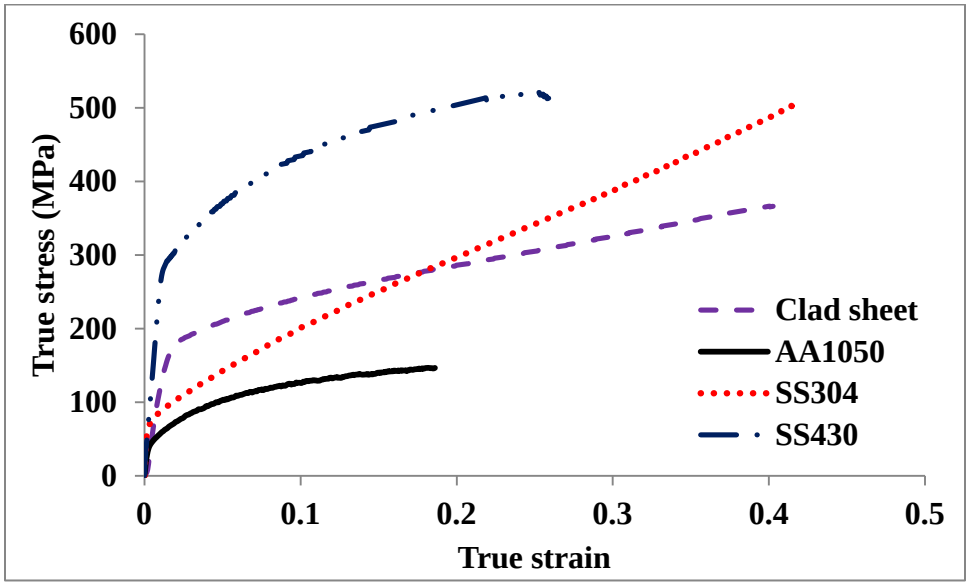

Fig. 5.3 A comparison of true stress-true strain plots

5.3 Forming limit diagram

The major and minor strains in the safe, necked and failure regions on the tested specimens as shown in Fig. 5.4 are measured and FLD is drawn such that strains at necking/fracture lie just at or above the line. The FLD of the clad sheet drawn on the basis of experimental data only is shown in Fig. 5.5. The measured limit strains would probably represent the maximum safe strains for these materials and the dome height at failure may be slightly less than the actual limiting dome height (LDH).

(a) **(b)**

Fig.5.4 (a) LDH Tested Specimens and (b) Necking/Failure zone on specimen

The stretch height is the punch stroke at which necking or a crack initiates in the sheet. The measured dome heights of various widths after punch stretching tests are given in Table 5.5. The minimum dome height of 18.04mm i.e. the FLD_0 in plane strain condition is observed in the sample with a width of 60mm and the corresponding major and minor strains are 0.325 and 0.067 respectively. The deformed sample shows both major and minor strains positive stating a condition of biaxial stretch (tension-tension) and hence the FLD_0 falls on right side of the plane strain condition. In all the cases of punch stretching experiments, the necking/ failure always occurred on the outer side of the dome i.e. AISI430 layer of the clad sheet. This could be contributed to the lower ductility of this material.

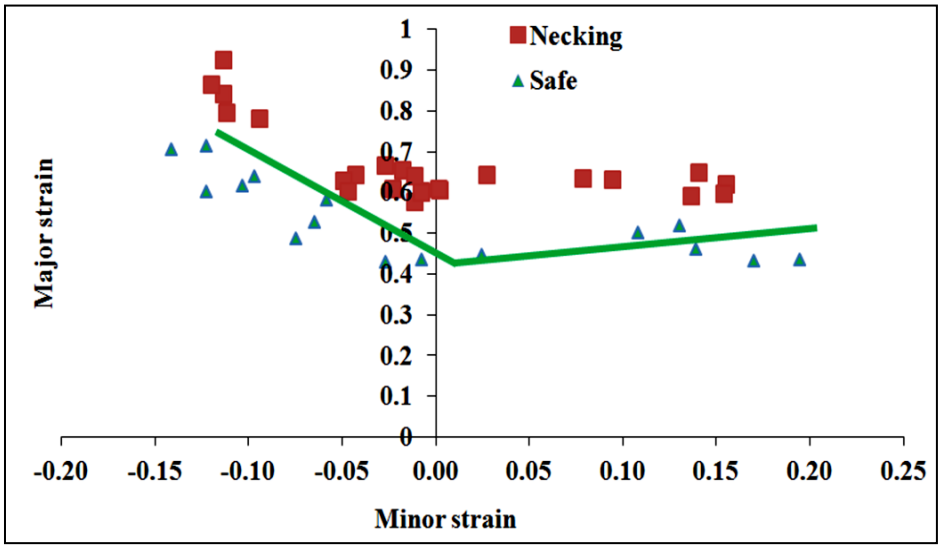

Fig. 5.5 Forming limit diagram for the clad sheet

Table 5.5. Comparison of experimental and predicted results

Sample width (mm)	Dome height at necking (mm)	Experimental critical strains		Predicted critical strains	
		Major	Minor	Major	Minor
20	25.06	0.879	-0.109	0.812	-0.128
30	24.33	0.583	-0.042	0.781	-0.053
40	24.98	0.649	-0.013	0.588	-0.012
50	24.39	0.670	0.012	0.471	-0.009
60	18.04	0.325	0.067	0.229	0.053
70	21.50	0.417	0.091	0.342	0.114
80	19.26	0.459	0.126	0.418	0.167
100	19.60	0.393	0.168	0.438	0.252

5.3.1 Numerical Simulations of Limit Dome Height test

The predicted critical strains (major and minor strains) after punch stretching simulations are also given in the Table 5.5. Highest strain values with a sample width of 20mm are predicted for a dome height of 25.06mm and these strain values decreases with the increase in the width of the sample till a plane strain condition is attained. The predicted values of critical minor strain and major strain are approximately zero and 0.471 respectively for a sample width of 50mm. As the width of the sample increases, both the strains become positive which indicates a biaxial stretch condition. The Stress contour, Minor critical strain contour, Major critical strain contour plots obtained during punch stretching test from FE analysis for a widths 20mm, 30mm, 40mm, 50mm, 60mm, 70mm, 80mm and 100mm are shown from Fig. 5.6 to Fig. 5.13.

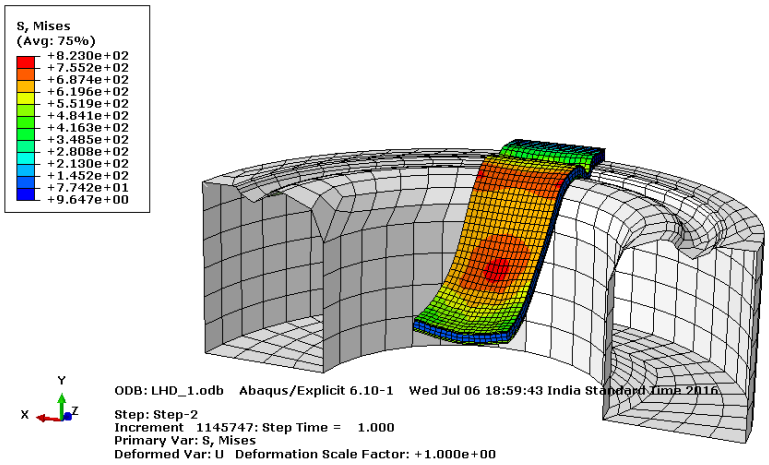

(a)

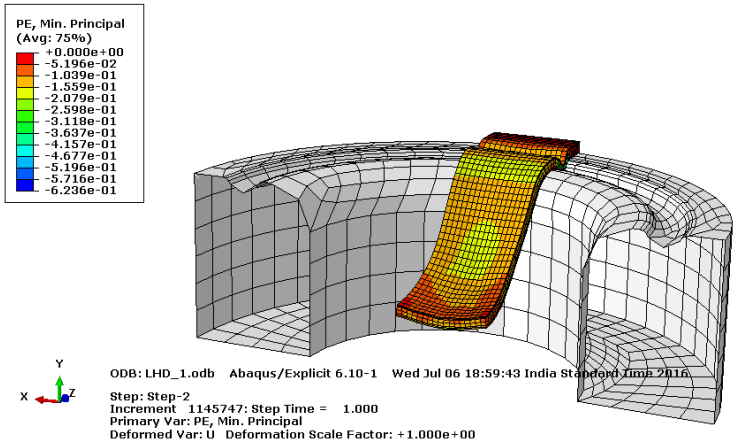

(b)

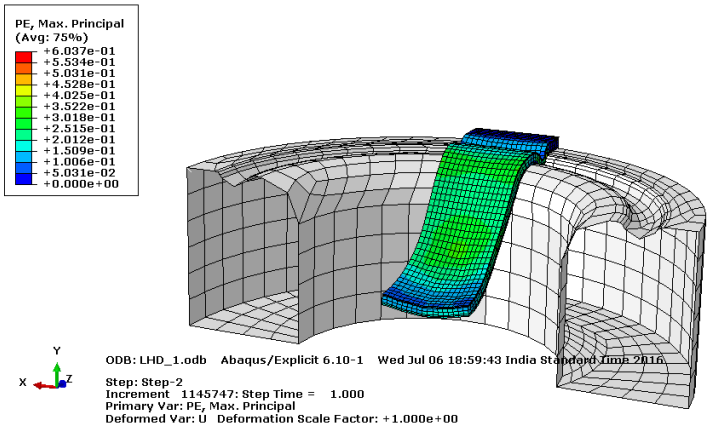

(c)

Fig 5.6 (a) Stress contour (b) Minor critical strain contour (c) Major critical strain contour; plots during punch stretching test for a width of 20mm

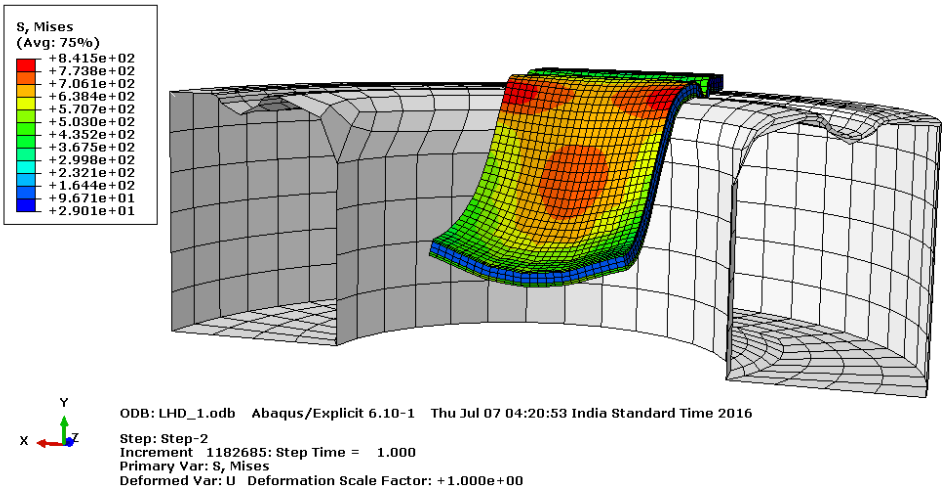

(a)

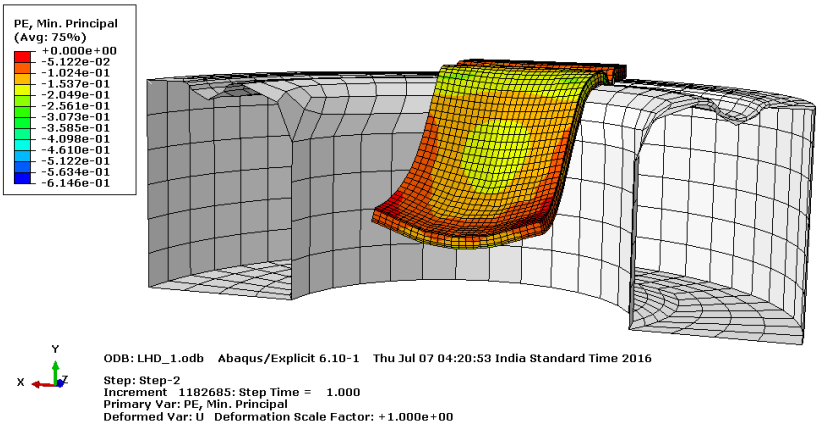

(b)

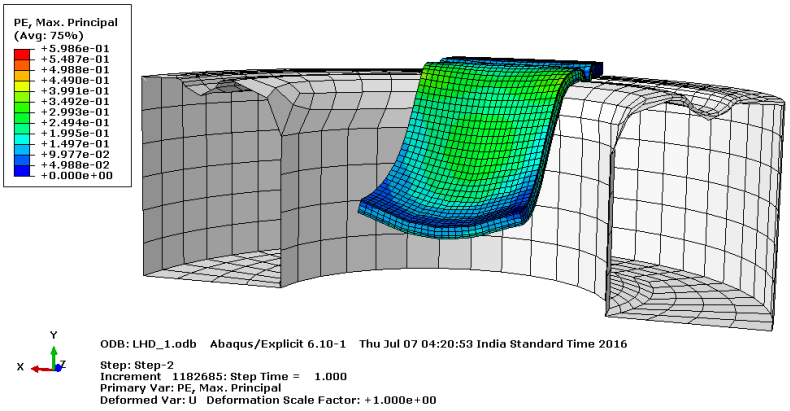

(c)

Fig 5.7 (a) Stress contour (b) Minor critical strain contour (c) Major critical strain contour; plots during punch stretching test for a width of 30mm

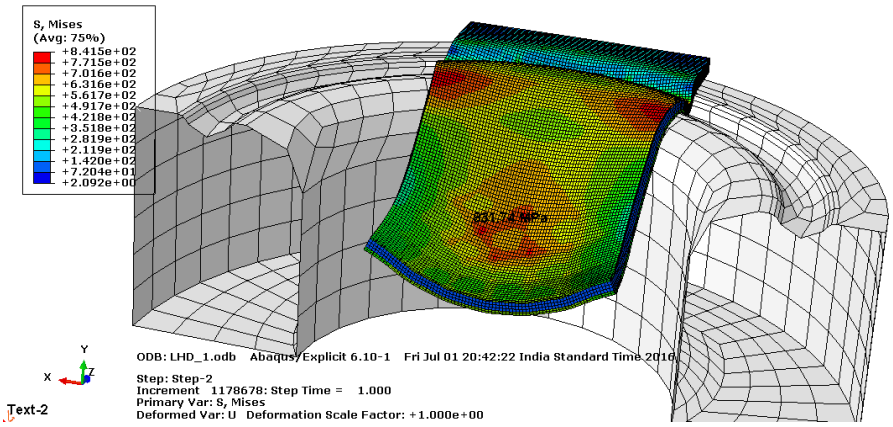

(a)

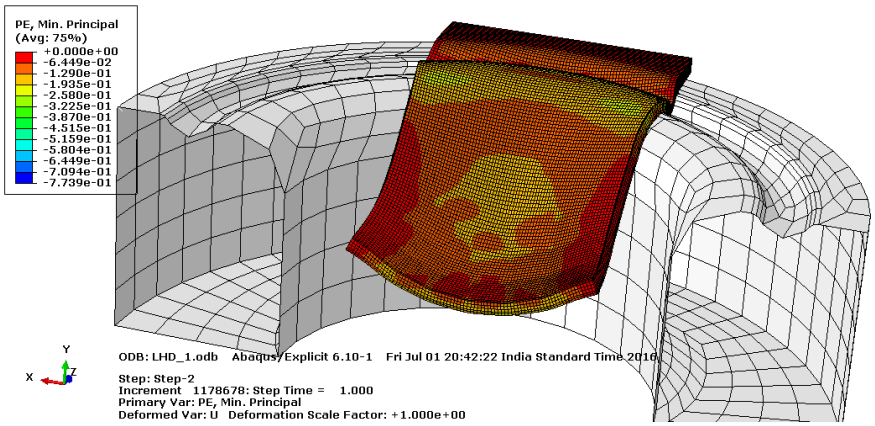

(b)

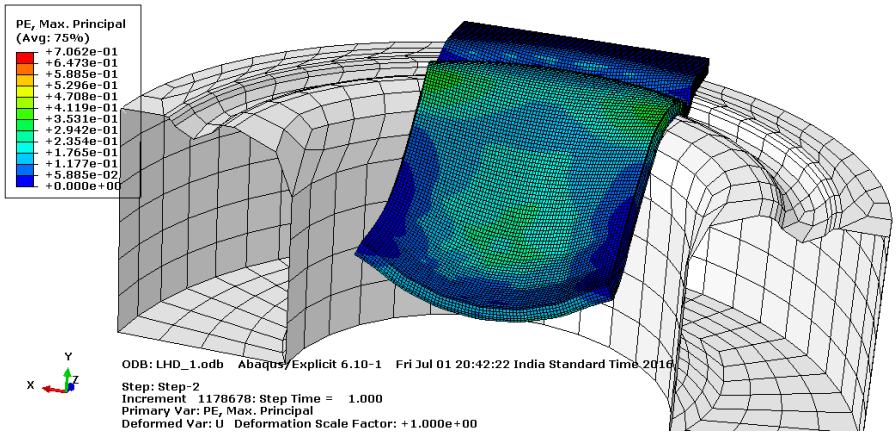

(c)

Fig 5.8 (a) Stress contour (b) Minor critical strain contour (c) Major critical strain contour; plots during punch stretching test for a width of 40mm

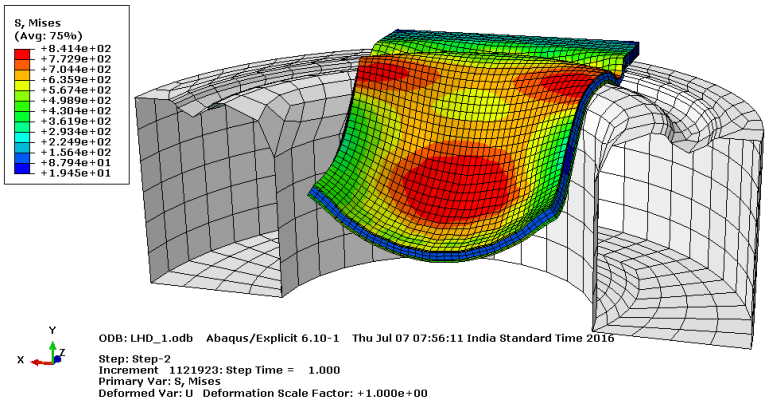

(a)

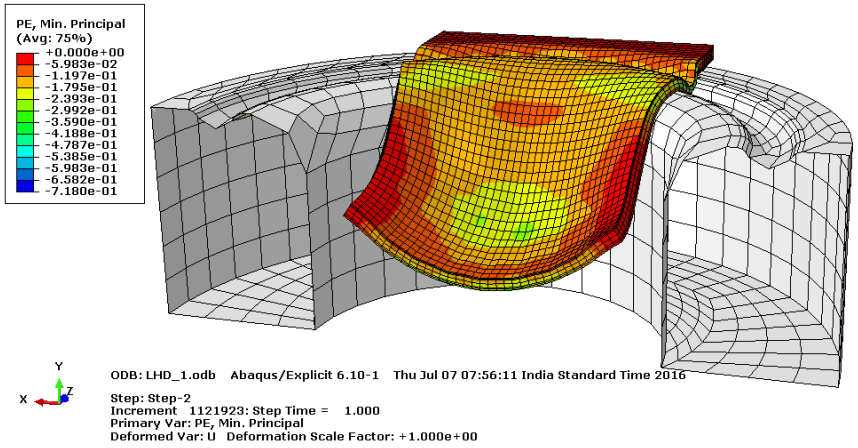

(b)

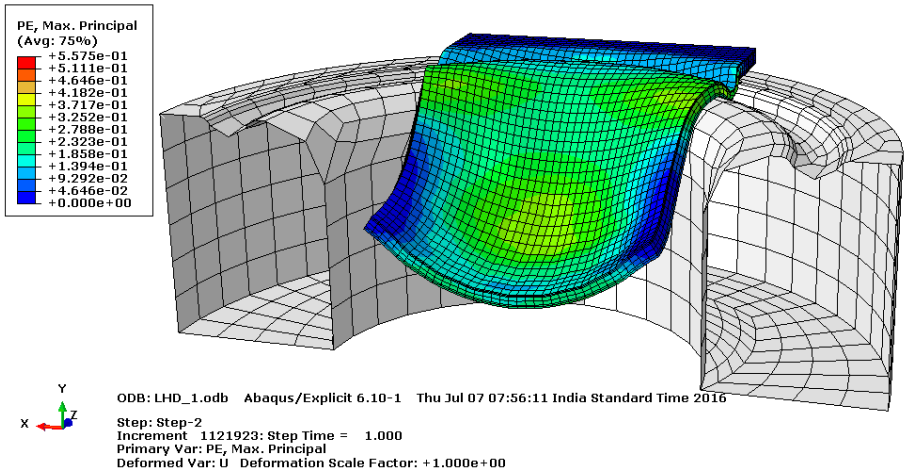

(c)

Fig 5.9 (a) Stress contour (b) Minor critical strain contour (c) Major critical strain contour; plots during punch stretching test for a width of 50mm

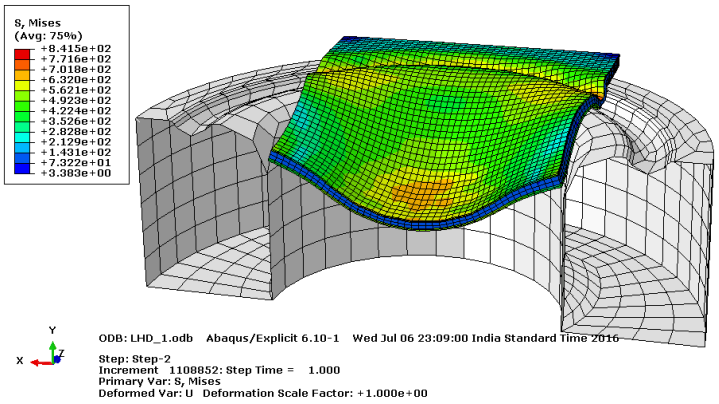

(a)

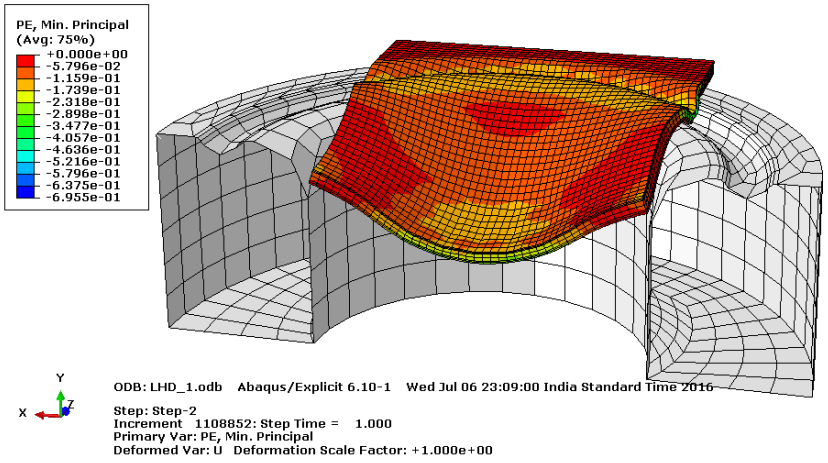

(b)

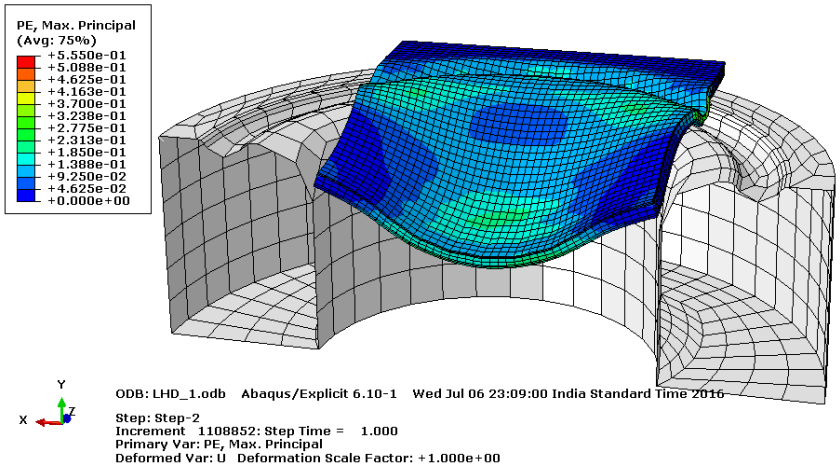

(c)

Fig 5.10 (a) Stress contour (b) Minor critical strain contour (c) Major critical strain contour; plots during punch stretching test for a width of 60mm

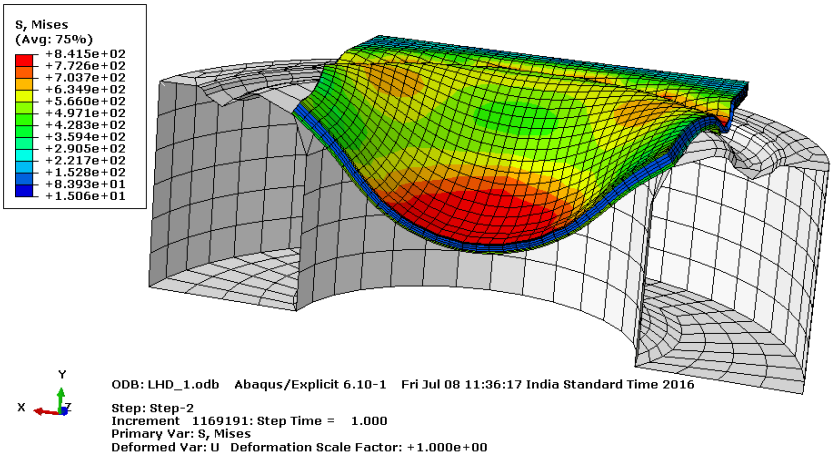

(a)

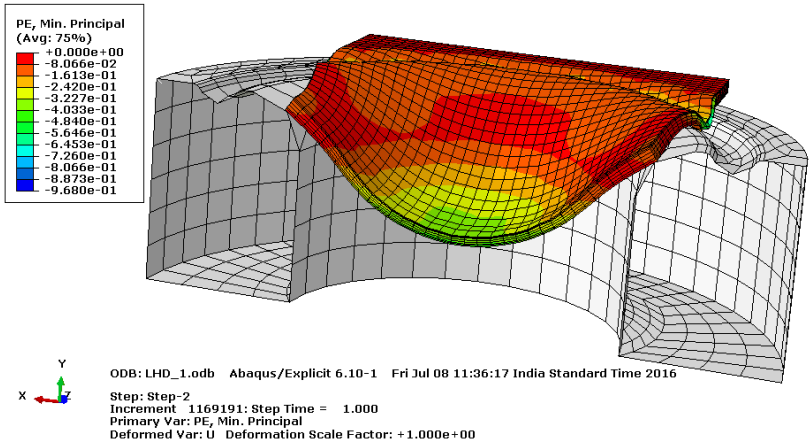

(b)

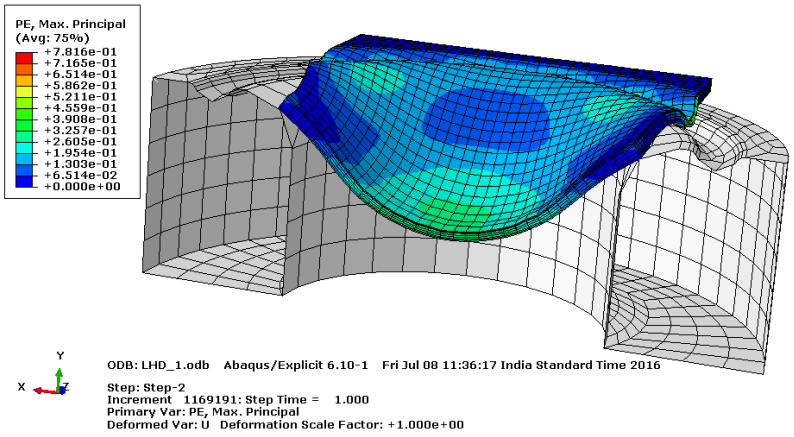

(c)

Fig 5.11 (a) Stress contour (b) Minor critical strain contour (c) Major critical strain contour; plots during punch stretching test for a width of 70mm

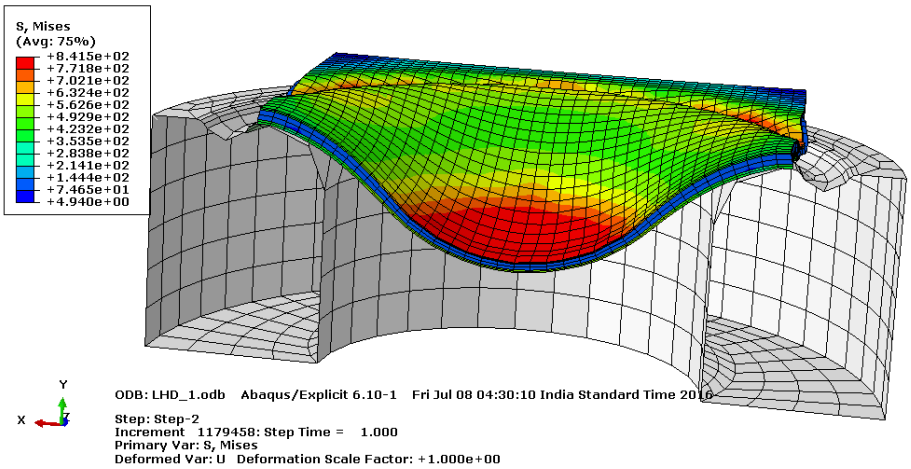

(a)

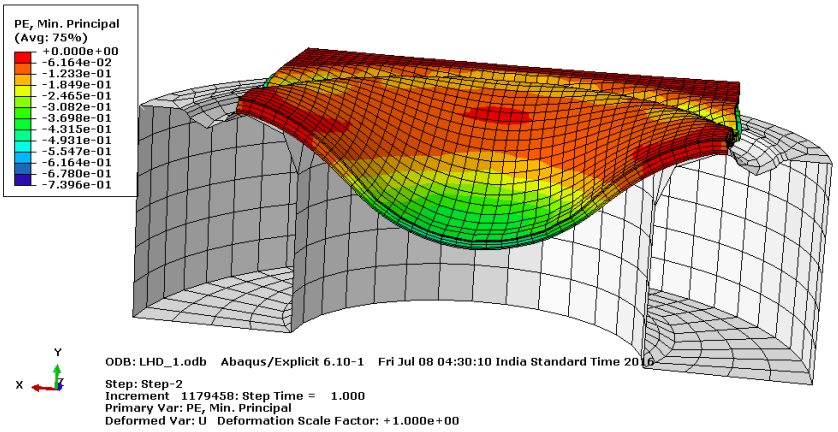

(b)

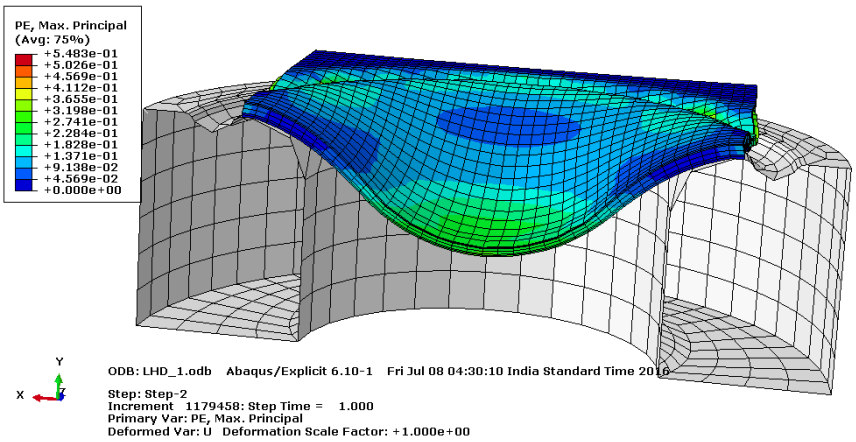

(c)

Fig 5.12 (a) Stress contour (b) Minor critical strain contour (c) Major critical strain contour; plots during punch stretching test for a width of 80mm

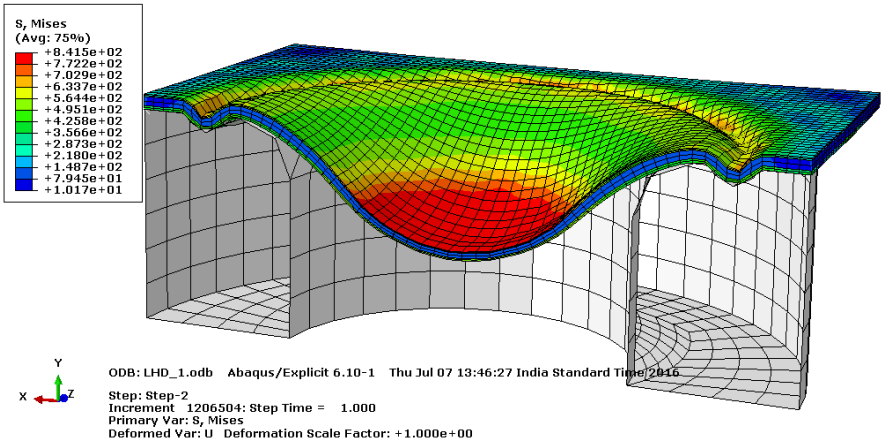

(a)

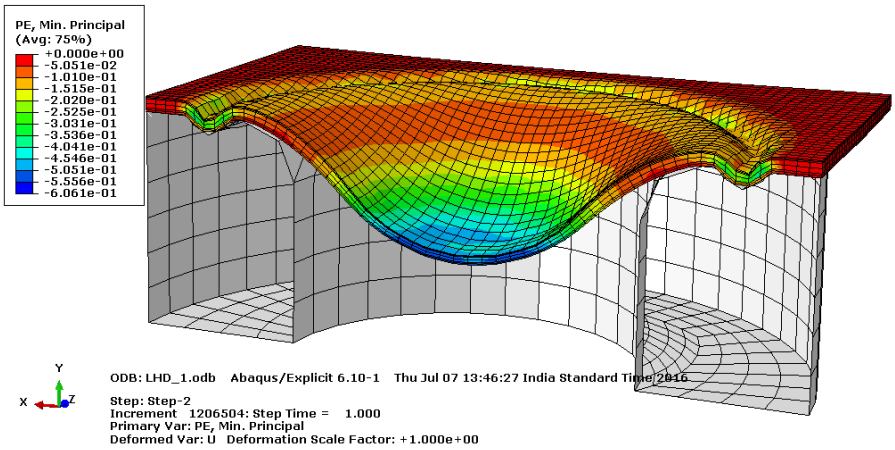

(b)

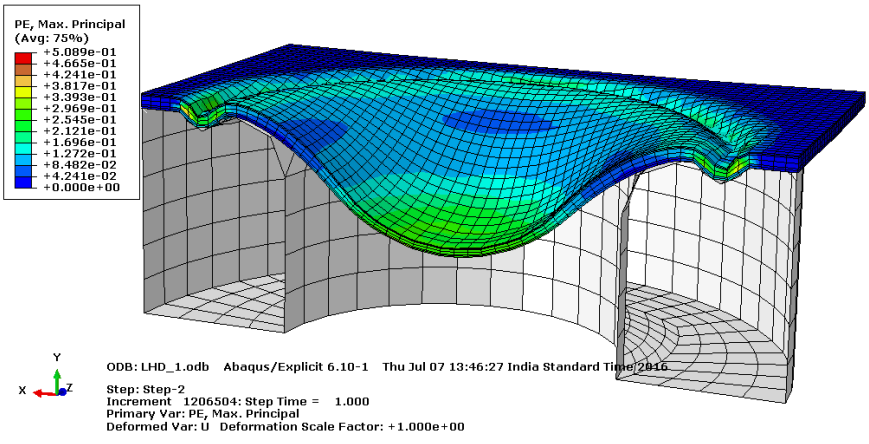

(c)

Fig 5.13 (a) Stress contour (b) Minor critical strain contour (c) Major critical strain contour; plots during punch stretching test for a width of 100mm

From the predicted results shown in Fig. 5.6 to Fig. 5.13, the necking/ failure of the clad sheet can be examined for a sample width of 20mm. It is seen that highest stress at the onset of failure is of order of 824 MPa and the corresponding major and minor critical strains are 0.812 and -0.128 respectively indicating the region of tension-compression during punch stretch test.

The plane strain condition was seen at the width of 50 mm where the highest stress at the onset of failure is of order of 840 MPa and the corresponding major and minor critical strains are 0.471 and -0.009(approximately zero) respectively.

The specimen at the widths above 50 mm showed state of biaxial stress state. The sample of width 100mm from the predicted results showed that the highest stress at the onset of failure is of order of 835 MPa and the corresponding major and minor critical strains are 0.438 and 0.252 respectively indicating the region of bi-axial stress state (tension-tension) during punch stretch test.

The Finite Element Analysis results for the punch stretch test are in close agreement with the experimental results as shown in Table 5.5.

CHAPTER - 6
CONCLUSIONS

The present study is focused on the tensile and forming behaviour of tri-ply SS304/AA1050/SS430 which is procured in annealed state. The following conclusions can be drawn:

1. The peeling strength of AISI304 is found to be 1.5 times higher than that of AISI430 on average basis. The peeling strength of AISI304 is in the range of 30 N/mm to 51 N/mm.
2. The peeling strength is seen to be increasing towards the end of the peeling distance which is due to the presence of shear deformation while preparation of the samples.
3. Tensile Behaviour of individual sheets show that AISI430 has higher tensile strength and appreciable value of strain hardening with lower ductility.
4. AISI304 has highest value of Strain hardening indicating more ductility and contributing excellent stretchability to the clad sheet.
5. AA1050 possesses lowest strength and ductility.
6. Tensile behaviour showed that the crack appeared first on AISI430 and then necking appears on AISI304, owing to its higher ductility.
7. The normal anisotropy of the clad sheet is less than one which indicates that it does not have good drawability.
8. Planar anisotropy of the clad sheet is very low indicating no earing defects in stretching operations.
9. The forming limit curve has been successfully drawn for the tri-ply clad sheet.
10. The minimum limiting dome height under plane strain condition appears at a width of 60mm, which is also verified by Keeler-Godwin FLD_0. The maximum dome height of 25.06mm was observed in samples width of 20mm.
11. The experimental FLD_0 in plane strain condition is observed in the sample with a width of 60mm and the corresponding minor and major strains are 0. 0.067 and 0.325 respectively.
12. The predicted values of critical minor strain and major strain are approximately zero and 0.471 respectively for a sample width of 50mm.
13. FEA results are in close agreement with the experimental results.

CHAPTER - 7
FUTURE SCOPES OF WORK

The work done in this thesis in the area of sheet metal forming to analyze the formability of a procured clad sheet of SS304/AA1050/SS430 can be further explored in various directions. Some of them which are listed as below:

1. The forming limit diagram(FLD) can be drawn for the other side of the sheet that is for AISI304 on bottom.
2. The cold roll bonding(CRB) of individual sheets can be done and heat treated, which will give us the actual condition of the produced clad sheet. This can reduce the gap between the results obtained from experimental and FE analysis.
3. The forming limit diagram(FLD) for the individual sheets can be drawn.
4. The effect of sheet thickness on FLD_0 can be analysed by conducting punch stretch test on clad sheet of varying thickness.

REFERENCES

1. Akbarzadeh, R. A. (2015). , Bond strength and mechanical properties of three-layered St/AZ31/St composite fabricated by roll bonding. *Materials & Design* , 880-888.

2. Dieter, G. E. (1988). *Mechanical metallurgy.*

3. Goodwin, G. (1968). Application of strain analysis to sheet metal forming problems in the press shop. *Society of Automotive engineers* , 380-387.

4. H. Danesh Manesh, A. K. (2003). Bond strength and formability of an aluminum-clad steel sheet. *Journal of Alloys and Compounds* , 138-143.

5. H.C.Tseng, C. H. (2010). An analysis of the formability of aluminum/copper clad metals with different thicknesses by the finite element method and experiment. *The International Journal of Advanced Manufacturing Technology* , 9-12.

6. H.R. Akramifard, H. ,. (2014). Cladding of aluminum on AISI304 Lstainless steel by cold roll bonding. *Materials Science & Engineering A613* , 232-239.

7. I.K. Kim, a. S. (2014). Mechanochemical joining in cold roll-cladding of tri-layered Cu/Al/Cu composite and the interface cracking behavior. *Materials & Design* , 625-631.

8. Keeler, S. P. (1961). *Plastic instability and fracture in sheet stretched over rigid punches.*

9. Kim, I.-K. a. (2013). Effect of component layer thickness on the bending behaviors of roll-bonded tri-layered Mg/Al/STS clad composites. *Materials & Design* , 935-944.

10. Lee, D. a. (1988). On the rule of mixtures for flow stresses in stainless-steel-clad aluminium sandwich sheet metals. *Journal of materials science* , 588-564.

11. Masoumi, M. a. (2013). Interface characterization and formability of two and three-layer composite sheets manufactured by roll bonding. *Materials & Design* , 392-396.

12. Miklós Tisza, Z. P. (2012). New methods for predicting the formability of sheet metals. *Production Processes and Systems* , 45-54.

13. N.V.Govindaraj, ,. J. (2013). Layer continuity in accumulative roll bonding of dissimilar material combinations. *Materials & Design* , 905-915.

14. Shi-Hoon Choi, K.-H. K. (1997). Tensile deformation behavior of stainless steel clad aluminum. *Materials Science and Engineering A222* , 158-165.

15. Yoshida, F. a. (1997). Forming limit of stainless steel-clad aluminium sheets under plane stress condition. *Journal of Materials Processing Technology* , 66-71.

16. Yu, J. a. (1997). Forming and failure behaviour of coated, laminated and sandwiched sheet metals: a review. *Journal of Materials Processing Technology* , 33-42.

17. thelibraryofmanufacturing.Retrievedfrom http://thelibraryofmanufacturing.com/rubberforming.htm

18. CustomPartNet. (2009). Retrieved from http://www.custompartnet.com/wu/sheet-metal-forming